Title

Signaling mechanisms and agricultural applications of (*Z*)-3-Hexenyl Butyrate-mediated stomatal closure

Authors

Celia Payá[1], Borja Belda-Palazón[1*], Francisco Vera-Sirera[1*], Julia Pérez-Pérez[1], Lucía Jordá[2,3], Ismael Rodrigo[1], José Mª Bellés[1], Mª Pilar López-Gresa[1] and Purificación Lisón[1].

[1]Instituto de Biología Molecular y Celular de Plantas (IBMCP), Consejo Superior de Investigaciones Científicas (CSIC), Universitat Politècnica de València (UPV), Ciudad Politécnica de la Innovación (CPI) 8 E, Ingeniero Fausto Elio s/n, 46011 Valencia, Spain

[2]Centro de Biotecnología y Genómica de Plantas (UPM-INIA), Universidad Politécnica de Madrid– Instituto Nacional de Investigación y Tecnología Agraria y Alimentaria (INIA), 28223. Pozuelo de Alarcón (Madrid), Spain

[3]Departamento de Biotecnología-Biología Vegetal, Escuela Técnica Superior de Ingeniería Agronómica, Alimentaria y de Biosistemas, Universidad Politécnica de Madrid. 28040 Madrid, Spain

*These 2 authors contributed equally to this work

Corresponding author: plison@ibmcp.upv.es

Running title

Mode of action and agricultural applications of the stomata closer (Z)-3-hexenyl butyrate

Highlights

(Z)-3-Hexenyl Butyrate closes stomata through activation of Ca2+ channels, mitogen-activated protein kinases and production of NADPH oxidase-mediated reactive oxygen species, in an abscisic acid independent manner, being proposed as a natural sustainable agrochemical against stresses.

Abstract

It is well known that plants respond to various stresses by releasing volatile organic compounds (VOCs). Green leaf volatiles (GLVs), which are commonly produced across different plant species after tissue damage, comprise an important group within VOCs. Among them, (*Z*)-3-hexenyl butyrate (HB) was described as a natural stomatal closure inducer, playing an important role in stomatal immunity, although its mechanism of action is still unknown. Here, through different genetic, pharmacological, and biochemical approaches we uncover that HB perception initiates different defense signaling events such as activation of Ca^{2+} permeable channels, mitogen-activated protein kinases (MPKs) and production of NADPH oxidase-mediated reactive oxygen species (ROS). Furthermore, HB-mediated stomata closure resulted to be independent of abscisic acid (ABA) biosynthesis and signaling. Additionally, exogenous treatments with this volatile alleviate water stress and improve fruit productivity in tomato plants. HB efficacy was also tested under open field conditions, leading to enhanced resistance against *Phytophthora* spp. and *Pseudomonas syringae* infection in potato and tomato plants, respectively. Collectively, our results provide insights into HB signaling transduction pathway, confirming its role in stomatal closure and plant immune system activation, and proposing HB as a new phytoprotector for the sustainable control of biotic and abiotic stresses in agriculture.

Keywords

Tomato, volatiles, stomata, bacteria, drought, (Z)-3-hexenyl butyrate,

Introduction

Plants have evolved a complex and efficient innate immune system to deal with pathogen attacks. Two different defensive layers are involved in plant immune responses (Jones and Dangl, 2006). The first line of plant innate immunity is established upon the recognition by receptors on the plasma membrane (pathogen recognition receptors; PRRs) of conserved microbial features, called as pathogen- and microbe-associated molecular patterns (PAMPs and MAMPs), activating the PAMP-triggered immunity (PTI) (Zhang & Zhou, 2010; Boutrot & Zipfel, 2017). At this level, plants are also able to perceive through different PRRs, molecules known as damage molecular patterns (DAMPs), released from plant cells upon pathogen attack. This

specific recognition trigger also a PTI response known as DAMP-triggered immunity (DTI) (Bjornson *et al.*, 2021). The second layer is started by the recognition of virulence factors, also called effectors, by intracellular receptors (nucleotide-binding, leucine-rich repeat receptors; NLRs), activating the effector triggered immunity (ETI) (Cui et al., 2015). Although both types of plant immune responses involve different activation mechanisms, PTI and ETI share many downstream components and responses, such as reactive oxygen species (ROS) production, increases in cytosolic calcium (Ca^{2+}) levels or activation of mitogen-activated protein kinases (MPK) cascades. Amplitudes and dynamics differ in each defensive level, postulating that ETI is an "accelerated and amplified PTI" (Yuan et al., 2021).

Many foliar pathogens, including bacteria, are unable to directly penetrate plant tissues and they use natural openings such as stomata that represent one of the most important passages for the entry of bacterial pathogens. As a countermeasure, plants have evolved a mechanism to rapidly close their stomata upon PAMPs/MAMPs perception limiting bacterial entrance, a defensive response known as stomatal immunity (Melotto et al., 2006). The bacterial MAMP flg22, an immunogenic epitope of the bacterial flagellin, is recognized by the PRRs receptor FLAGELLIN-SENSITIVE2 (FLS2) and the coreceptors BRI1-ASSOCIATED RECEPTOR KINASE1 (BAK1) and BOTRYTIS-INDUCED KINASE 1 (BIK1) (Gómez-Gómez & Boller 2000; Chinchilla et al., 2006; Chinchilla et al., 2007; Kadota *et al.* 2014). This recognition by the FLS2 complex triggers a cascade of signaling events including increases of Ca^{2+} influx, ROS burst through the activation of plant NADPH oxidases, MAPK cascades and activation/inhibition of ion channels, all leading to stomatal immunity (Arnaud and Hwang, 2015).

The phytohormone abscisic acid (ABA) is essential in stomatal defense during plant immunity (Bharath *et al.*, 2021). In fact, ABA-induced stomatal closure shares a common signaling pathway with PAMP-induced stomatal closure, including ROS burst, nitric oxide (NO) intermediate accumulation, activation of S-type anion channels, or the inhibition of K^+ channels (Arnaud and Hwang, 2015). Besides, both signals converge at the level of open stomata 1 (OST1), a serine/threonine protein kinase also known as SnRK2.6 that activates S-type anion channels like the slow anion channel-associated 1 (SLAC1) and SLAC1 homolog 3 (SLAH3), and the R-/QUAC-type anion channel QUAC1 (Mustilli et al., 2002; Vahisalu et al., 2008; Montillet et al., 2013) (Chong *et al.*, 2022). Despite this, there are some differences in the canonical stomatal immunity signaling components in both PTI and ABA signaling pathways. ABA-induced ROS

production depends on the kinase OST1, which phosphorylates and activates RBOHF/RBOHD. However, during PTI stomatal closure, ROS are produced by the activation of the NADPH oxidase RBOHD that is directly phosphorylated by the plasma-membrane-associated kinase BIK1 (Kadota *et al.*, 2014; Arnaud and Hwang, 2015). Furthermore, MPKs are known to play a specific role in stomatal immunity. MPK3 and MPK6 positively regulate flg22-trigered stomatal closure in a partially redundant manner, but they are not involved in ABA-mediated stomatal closure (Montillet et al., 2013; Su et al., 2017). Intriguingly, MPK9 and MPK12 act redundantly as positive regulators of ABA- and ROS-mediated stomatal immunity, acting downstream of ROS production and Ca^{2+} fluxes, while they seem not to be involved in the flg22-induced stomatal closure (Jammes et al., 2009, 2011). It has been also reported that not only JA through the phytotoxin coronatine which is produced by various strains of *Pseudomonas syringae*, but also ABA mediate the inactivation of the MPK3 and MPK6, promoting *Pseudomonas syringae* DC3000 pv. *tomato (Pst* DC3000*)* virulence. Moreover, to counteract bacterial suppression of MAPKs, host plant block JA signaling pathway upon ETI establishment (Mine *et al.*, 2017).These results demonstrate the highly interconnected network of plant immune signaling pathways, and how it can be exploited by host plants and pathogens.

After pathogen invasion, plant metabolic pathways are dramatically reprogrammed, triggering the accumulation of a plethora of secondary metabolites to cope with this stress. The defensive metabolites may act through direct mechanisms as antimicrobial or antifungal agents *per se,* or through indirect mechanisms, participating in the signaling/amplification of the plant defense responses. Due to its gaseous nature, volatile organic compounds (VOCs) act as fast signaling molecules that activate plant defensive response pathways between distant organs, and they even allow communication between different plants (Baldwin et al., 2006; Heil & Bueno, 2007; Dudareva et al., 2013). Several studies have demonstrated that VOCs are able to induce defenses against herbivorous insects, pathogens, and even environmental stresses (Baldwin et al., 2006; Ameye et al., 2015; Cofer et al., 2018; Brilli et al., 2019). Defense priming against pathogens induced by VOCs has been considered as a sort of “green vaccination” (Luna 2016; Brilli et al., 2019).

A non-targeted GC-MS metabolomics analysis revealed the VOCs profile associated with the immune response of tomato cv. Rio Grande plants upon infection with either virulent or avirulent strains of the model bacterial pathogen *Pst* DC3000*.* In the case of the avirulent infection which leads to the establishment of ETI, the VOC profile of

immunized plants was characterized by esters of (*Z*)-3-hexenol with acetic, propionic, isobutyric or butyric acids, and several monoterpenoids such as linalool or α-terpineol (López-Gresa *et al.*, 2017). The defensive role of these compounds was tested trough exogenous application in tomato plants and, among all these compounds, treatments with (*Z*)-hexenyl butyrate (HB) resulted in the transcriptional upregulation of defensive genes, stomatal closure and enhanced resistance to the bacterial infection with *Pst* DC3000, confirming the role of HB as a natural defense elicitor (López-Gresa et al., 2018). Additionally, HB-mediated stomatal closure was effective in different plant species, which also led to accelerated ripening in *Vitis vinifera* (López-Gresa et al., 2018; Payá et al., 2020).

In this study, we investigated the signaling mechanisms underlying HB-mediated stomatal closure and plant immunity. The results showed that HB triggers stomatal closure not only in an ABA-independent manner, but through Ca^{2+}, ROS and MAPK-signaling cascade activation. Furthermore, we tested the efficacy of this compound in water stress and its effectiveness was also assessed against both biotic and abiotic stresses under field conditions. Taken together, we propose a new role for HB as a natural elicitor against biotic and abiotic stresses.

Materials and Methods

In this study *Solanum lycopersicum* (tomato) var. MoneyMaker were used. Tomato ABA-deficient mutants *flacca (flc)* (Taylor *et al.*, 1988) and their corresponding parental Lukullus plants, were kindly provided by Dr. Jorge Lozano (IBMCP, Valencia, Spain). Tomato seeds were chemically sterilized with a 1:1 mixture of sodium hypochlorite and distilled water. After sterilization, seeds were placed in 12 cm-diameter pots containing vermiculite:peat (1:1). Plants were grown under greenhouse conditions with 16/8 h (24/18 °C) photoperiod and a relative humidity between 50-70%.

In the case of greenhouse drought experiments, water stress was simulated by quitting irrigation during 6 days in the case of stressed plants, whilst control plants were normally watered. HB-treatments were performed every 2 days, until the end of the experiments.

Arabidopsis thaliana were also employed. All the Arabidopsis plants were in Columbia (Col-0) ecotype background. *mpk3* and *mpk6* mutants were kindly provided by Dr. Borja Belda-Palazón (IBMCP, Valencia, Spain). Plants were grown in a chamber under

short-day conditions (10/14 h; 19/23 °C light/darkness), with a relative humidity ranging from 50 to 60%.

HB treatments under greenhouse conditions

Treatments were carried out on 4-week-old tomato plants either in closed chambers or by spray. Tomato plants were placed into 121 L methacrylate chambers containing hydrophilic cotton swabs soaked with 5 μM of (*Z*)-3-hexenyl butyrate (HB; Sigma-Aldrich, Saint Louis, MO, USA) or distilled water in the case of control plants. Methacrylate chambers were hermetically sealed during the 24 h treatment. In the case of spray treatments, tomato plants were pre-treated by spray with HB at a concentration of 2 mM or distilled water (mock), containing 0.05% Tween 20 as wetting agent.

Bacterial inoculation assays

The bacterial strain used in this study was *Pst* DC3000 (kindly provided by Dr. Selena Gimenez, Centro Nacional de Biotecnología, Madrid, Spain). Bacteria were grown in LB agar medium supplemented with rifampicin (10 mg/mL) and kanamycin (0.5 mg/mL) during 48 h at 28 °C. An independent colony was transferred into King's B liquid medium containing rifampicin and grown at 28 °C. After 48 h, bacteria were centrifuged and resuspended in 10 mM sterile $MgCl_2$ to an OD_{600}=0.1, which corresponds to a final inoculum concentration of 5×10^7 CFU/mL approximately. For spray inoculation assays on Arabidopsis plants, a *Pst* DC3000 suspension (OD_{600}=0.2) was prepared in 10 mM $MgCl_2$ containing 0.05% Silwet L-77, and sprayed onto 4-week old plants. The bacterial growth experiments were carried out by sampling three leaf discs (1 cm^2 each) from each plant at 72 hours post inoculation. Tissue samples were ground in 10 mM $MgCl_2$, serial dilutions were done and plated on Petri dishes containing King's B medium supplemented with rifampicin. Bacterial colonies were counted 48 h after serial dilutions.

Stomatal aperture measurement

To measure stomatal aperture in tomato plants, clear nail polish was applied in the abaxial part of five leaves from three independent plants. Once the film was dry, it was carefully peeled off and leaf impressions were obtained.

In the case of leaf discs, they were taken from 3- to 4-week old plants and floated on Murashige & Skoog medium (MS) for 3 h under light, in order to induce stomatal opening. Then, stomata closing elicitors (HB, ABA and flg22) were added to the medium at the appropriated concentration for 3 h. For chemical inhibitors, 2 mM salicylhydroxamic acid (SHAM), 20 μM diphenyleiodonium chloride (DPI), 2 mM EGTA and 20 μM PD980059 were added 30 minutes before incubation with the elicitors.

In both cases, samples were then visualized under a Leica DC5000 microscope (Leica Microsystems GmbH, Wetzlar, Germany) and pictures of different regions were analyzed with *ImageJ* software. Aperture ratio was measured as stomata width/length from at least 50 stomata per plant and/or treatment, considering a value of 1 as a totally opened stomata.

Ion leakage estimation

Five leaf discs (1 cm^2) were excised using a stainless steel cork borer, then immersed in tubes containing 40 mL of deionized water and shaken at 200 rpm for 2 h at 28°C. The conductivity of the solution (L1) was measured with a conductivity meter (DDS-11A, Shanghai Leici Instrument Inc., Shanghai, China). After that, the solution was boiled for 15 min, cooled to room temperature, and the conductivity of killed tissues (L2) was measured. Ion leakage was calculated as the ratio of L1 to L2.

RNA isolation and RT-qPCR analysis

Total RNA of tomato leaves was extracted using TRIzol reagent (Invitrogen, Carlsbad, CA, USA), following the manufacturer's protocol. RNA was then precipitated by adding one volume of 6 M LiCl and keeping it on ice for 4 h. Afterward the pellet was washed using 3 M LiCl and was dissolved in RNase-free water. Finally, in order to remove any contaminating genomic DNA, 2 U of TURBO DNase (Ambion, Austin, TX, USA) were added per microliter of RNA. For the quantitative RT-qPCR analysis, one microgram of total RNA was employed to obtain the corresponding cDNA target sequences using an oligo$(dT)_{18}$ primer and the PrimeScript RT reagent kit (Perfect Real Time, Takara Bio Inc., Otsu, Shiga, Japan), following the manufacturer's directions. Quantitative PCR was carried out as previously described (Campos et al., 2014). The housekeeping gene transcript actin was used as the endogenous reference. The PCR primers were designed using the online service Primer3 (https://primer3.ut.ee/) and are listed in Supplemental Table 1.

RNA-Seq and GO analyses

Six individual MoneyMaker tomato plants of 4 weeks-old were placed into methacrylate chambers and treated with HB or distilled water as described above. Twenty-four hours post-treatments leaves samples were collected and total RNA was extracted and analyzed using an 2100 Agilent Bioanalyzer (Agilent Technologies, Inc., Santa Clara, CA, USA) to check RNA integrity and quality. RNA-Seq and bioinformatics analysis were performed by Genomics4All (Madrid, Spain). Samples were sequenced with x50 tomato genome coverage using 1 x 50 bp reads. Raw data was aligned to *Solanum lycopersicum* genome using HISAT2 v2.1.0 (Kim et al., 2015). StringTie was used to obtain the differential expression (Pertea et al., 2015). Data and transcript-level expression analysis, and functional enrichment analysis were performed following previously described protocols (Pertea et al., 2015, 2016; Kovaka et al., 2019; Raudvere et al., 2019). GO enrichment analysis were performed with Panther Classification System (http://pantherdb.org) (Mi et al., 2019).

MPK phosphorylation assay

Leaf discs were taken from 3- to 4-week-old tomato and *Arabidopsis thaliana* plants and floated on MS medium for 3 h under light. Then, flg22 1 μM, ABA 10 μM and HB 50 μM treatments were performed, and samples were taken 15, 30 and 60 minutes after treatments, and immediately frozen in liquid nitrogen. Frozen leaf samples were homogenized and proteins extracts were obtained by Laemmli extraction method. Briefly, leaf disc powder (100 mg) was mixed with 150 µL 2x Laemmli buffer and incubated on ice for 20 min, vortexing every 5 min. Samples were thereafter boiled for 10 min, cooled on ice for 5 min, and centrifuged at 12000 x *g* for 5 min at 4 °C to clarify homogenates. The resulting supernatants (10 µL) were analyzed by Western Blot with Phospho-p44/42 MAPK (Erk1/2) (Thr202/Tyr204) (Cell Signaling, 1679101S; dilution 1:1,000) primary antibodies, and peroxidase-conjugated goat anti-rabbit IgG (Jacksons, 111035144; dilution 1:20,000) secondary antibodies.

Open-field HB treatments

Abiotic stress

This assay was carried out at Picanya, located in Valencia, Spain (39°26′08″N, 0°26′09″O). Due to the volatility of the compound, the field trial was performed in two

independent greenhouses, one for HB treatments and the other one for control treatments. The experimental design used was randomized blocks (9 m^2) with 4 biological replicates per treatment. Plants were sprayed with 5 mM HB every two weeks. To provoke water stress, irrigation was completely stopped. The soil capacity was continuously monitored and once it reached 50%, the water regime was re-established. Different parameters like number of flowers, fruit set, and total fruits as well as fruit weight were assessed. Moreover, at harvest, total yield was analyzed per categories as follows: small size (25-50 mm diameter, 25-100 g weight); medium size (50-75 mm diameter,100-200 g weight); big size (75-100 mm diameter, 200-300 g weight); and extra size (>100 mm diameter, >300 g weight).

In all the field trials, time units are referred as follows: X DA Z, being X day (0-18); DA Days After; Z day of treatment (A-H).

Abiotic stress trials were performed under General Standards, in accordance with EPPO Guidelines PP 1/153(4), PP 1/181(4), PP 1/135 (5) and PP 1/239(2).

Biotic stress

The trial of tomato plants inoculated with *Pseudomonas syringae* was performed under open field conditions in Torrellano (Alicante, Spain, 38°17′39″N, 0°35′11″O). The tomato plants were transplanted on August 26th, 2020 and the commercial variety Muchamiel was used. The experiment comprised 6 plots (10 plants each) treated with HB at 0.05, 5, 10, and 50 mM, plus another plot that was treated with the commercial pesticide OXICOOP 50 as a positive control, and one plot was left untreated. Treatment applications were carried out using a motorized knapsack sprayer. Three applications were carried out, the application A being preventive and subsequent applications (B and C) were carried out with 6 to 8 days interval coinciding with the persistence of the effect of HB (López-Gresa et al., 2018).

To determine the efficacy of HB for the control of *Downy mildew* in potatoes, an independent open field condition trial was performed in Borbotó (Valencia, Spain, 39°30′55″N, 0°23′27″O). The potato plants were transplanted on February 18th 2019 and the variety used was Vivaldi. The experimental design used was randomized block with 6 plots (one plot per treatment) and 60 plants in each one. Foliar treatments were performed following the same methodology and strategy than in the case of the tomato experiment, but in this case ORO-COBRE ZINEB was used as positive control. Four applications were carried out, being application A before disease appears, and following applications (B, C and D) with 7±1 days intervals.

In both experiments, the degree of infection was assessed as percentage of leaves presenting symptoms (incidence) and percentage of infected leaf area per diseased leaf (severity). The efficacy (E) of the treatments was calculated according to the Abbott's formula (Abbott, 1925), using the percentage of leaf area affected in control (C) and treated (T) groups. The following formula was used:

$$E = \frac{(C - T)}{C} \times 100$$

Tomato and potato-pathogen inoculation trials were performed in accordance with EPPO (Efficacy evaluation of Plant protection Products) guidelines PP1/135(4), PP1/152(4) and PP1/181(4), and specific EPPO PP1/2(4).

Statistical analysis

The statistical analysis of two or more variables was carried out by using Student's *t*-test or analysis of variance (ANOVA), respectively employing the GraphPad's Prism 9 software. In all the analyses, a *p*-value <0.05 was considered statistically significant.

Results

Treatments with HB induce transcriptomic changes related to plant immunity and photosynthesis

To provide insight into the molecular mechanisms underlying the tomato plant response to HB, an RNA-seq analysis was performed on leaves tissues from mock and HB-treated tomato plants. After trimming and filtering data, a total of 1456 genes were found to be differentially expressed (DEGs) between HB- and control-treated plants (DEG threshold= 2), indicating that HB treatments produce an outstanding effect at the transcriptional level. To classify DEGs, a GO enrichment analysis for biological processes (BP), cellular components (CC) and molecular functions (MF) was performed for up- and down-regulated DEGs, independently.

Among the upregulated genes, 1122 DEGs were annotated being the BP category the most enriched one (Figure 1A). In this regard, most of the DEGs were putatively involved in organonitrogen compound metabolic processes (GO:1901564), chitin metabolic process (GO:0006030) or amino glycan and amino sugar metabolic processes (GO: 0006040, GO:0006022). MF category included chitinase activity (GO:0004568), chitin binding (GO:00080761) or endopeptidase activity (GO: 0004175),

which are mainly related to pathogen defensive responses. On the other hand, only 334 downregulated DEGs were annotated, and most of them were associated with the CC category mainly related to plastoglobule (GO:0010287), photosystem (GO:0009521) and chloroplast (GO:0009507) (Figure 1B). Indeed, the most enriched groups when biological processes were assessed were related to photosynthesis (GO:0015979) and the only enriched MF term was chlorophyll binding (GO:0016168). Both defensive- and photosynthesis-related gene expression were confirmed by RT-qPCR (Supplemental Figure 1), observing a statistically significant induction for the pathogenesis-related genes *PR1* (X68738) and *PR5* (X70787), as well as a gene coding for a putative PRR immune leucine-rich repeat receptor-like kinase (Solyc12g036793) and also a gene involved in heavy metal resistance and detoxification (Solyc06g066590). Besides, a reduction in the expression of genes encoding chlorophyll binding proteins (Solyc06g069730; Solyc06g069000; Solyc12g011280) was also validated. Therefore, RNA-seq transcriptomic analysis revealed that HB treatments induced plant defensive responses against pathogens as well as photosynthesis reprogramming.

ROS production via NADPH oxidases and Ca^{2+} signaling but not ABA are required for HB-mediated stomatal closure

To decipher the signaling pathway by means of which HB mediates stomatal closure, an appropriate method was developed for stomatal measurement analyses (Materials and Methods). In these experiments, we studied the effect of HB in comparison with the positive controls for stomatal closure flg22 and ABA, considering both dose-response and time-course assays of these compounds to optimize the different treatments (Supplemental Figure 2). Once set up, we studied whether ABA was necessary for the HB-dependent stomata closure. For this purpose, we took advantage of both *flacca* (*flc*) tomato mutants that are impaired in ABA biosynthesis and their corresponding parental Lukullus wildtype (WT) plants (Tal, 1966). As expected, HB, flg22 and ABA treatments promoted stomatal closure in WT plants. In *flc* mutants, the stomatal aperture ratio in mock conditions was significantly higher compared to WT plants, probably due to a reduction of the ABA levels. However, ABA treatments in *flacca* mutants closed the stomata to the same extent than flg22 and HB, suggesting that ABA biosynthesis is not required for flg22- and HB-mediated stomatal closure (Figure 2A).

As aforementioned, Ca^{2+} and ROS also play a pivotal role in the stomatal response, acting as secondary messengers upon pathogen attack. Therefore, we decided to analyze the role of these signaling molecules in the HB-mediated stomatal closure. For this purpose, we performed pre-treatments with the specific Ca^{+2} ion chelator EGTA (ethylene-bis(oxyethylenenitrilo)tetraacetic acid), and the ROS production inhibitors DPI (Diphenyleneiodonium, which inhibits NADPH oxidase) or SHAM (salicylhydroxamic acid, acting on peroxidases) before triggering the stomatal closure with either HB, flg22 or ABA. Pre-treatments with EGTA completely abolished the stomatal closure mediated by all, HB, flg22 and ABA treatments, indicating that Ca^{2+} signaling is essential for stomatal closure (Figure 2B). Interestingly, pre-treatments with DPI partially abrogated the stomatal closure induced by HB, flg22 and ABA, suggesting that NADPH-dependent ROS production is partially necessary for this process (Figure 2C). However, unlike flg22 and similar to ABA treatments, SHAM did not inhibit HB-induced stomatal closure, indicating that stomatal closure promoted by HB is independent of ROS production by peroxidases (Figure 2D).

Our results seem to indicate that HB-mediated stomatal closure requires Ca^{2+} fluxes and is partially dependent on ROS generation by NADPH oxidases but is nevertheless independent of ABA biosynthesis and ROS generated through peroxidases.

Activation of MPK3 and MPK6 is essential for HB-mediated stomatal immunity

To test whether HB intracellular signaling occurs through activation of MPK-cascades, we analyzed the phosphorylation of MPK3 and MPK6 in tomato and *Arabidopsis thaliana* leaf discs after treatments with flg22, ABA and HB. Regarding tomato samples, 15 minutes after treatments HB induced MPK3 phosphorylation, and this activation persisted until 60 minutes after treatments (Figure 3A). Nevertheless, in *Arabidopsis thaliana* samples MPK3/6 phosphorylation was observed at 60 minutes after HB treatments, suggesting that MPKs activation phenomenon occurs earlier in tomato than in *Arabidopsis thaliana* plants (Figure 3B).

To confirm the importance of MPK3/6 activation in HB-mediated stomatal immunity, pre-treatments with the MPKs inhibitor PD98059 on tomato leaf discs were performed. After PD98059 application, flg22, ABA and HB treatments diminished their ability to induce stomatal closure, confirming that MAPKs play a pivotal role in all the elicited stomatal responses (Figure 3C). Furthermore, treatments with PD98059 were also carried out *in planta* (see Materials and Methods). In this regard, application of

PD98059 diminished HB enhanced resistance to bacterial infection (Figure 3D). These results indicated that HB induces stomatal immunity partially via activation of the MPK3/6 signaling cascades in tomato plants, without discarding that other mechanisms should also be involved in the HB-mediated stomatal immunity.

To better characterize this, a genetic approach in *Arabidopsis thaliana mpk3* and *mpk6* mutants was performed. To do this, the stomatal behavior was analyzed as described in Materials and Methods. As expected, ABA treatments reduced dramatically stomatal aperture in both Arabidopsis mutants and WT plants. In contrast, and in accordance with chemical inhibitor experiments performed in tomato plants, stomata aperture ratio was identical to that observed in mock-treated plants not only in flg22- but also in HB-treated *mpk3* and *mpk6* mutants, whilst treatments were efficient in the corresponding WT Arabidopsis plants (Figure 3E). The incapacity of HB in closing stomata in *mpk3* and *mpk6* mutants resulted in non-enhanced resistance to bacterial infection with *Pst* after HB treatments (Figure 3F).

Additionally, the expression of MPK3/6 target genes was also explored upon HB treatment. As shown in Figures 4A and 4B, HB treatments of tomato plants significantly induced *SlWRKY33A* and *SlWRKY33B* transcription factors, which correspond to tomato orthologs of *AtWRKY33.* This gene has been described to work downstream of MPK3/MPK6 in the reprogramming of the expression of genes involved in camalexin biosynthesis and pipecolic acid in Arabidopsis (Mao et al., 2011; Zhou et al*.,* 2015; Wang et al., 2018). Since MAPK3/6 seem to play a central role in the regulation of the ethylene response pathway (Hahn and Harter, 2009), ethylene signaling-related genes like the ethylene receptor ETR4 and an ethylene responsive factor (ERF) were also analyzed, observing a significant induction of the expression of both genes (Figures 4C and 4D). Taken together, these results indicate that MPK3/6 are involved in HB-mediated stomatal immunity.

HB treatments confer drought tolerance in tomato

The robust effect of HB in promoting the closure of stomata prompted us to study the effect of HB on drought tolerance. To that purpose, well-watered as well as drought-stressed tomato plants were periodically treated with HB and stomatal opening and closing dynamics were monitored. Three days after drought exposure (DAD), stomatal aperture ratio in HB-treated plants was lower than in control-treated plants, confirming the role of HB as stomatal closure inducer in tomato plants, even in drought conditions. It should be noted that HB treatments in well-watered conditions caused similar

stomatal closure to those control-treated plants subjected to drought. Moreover, at 6 DAD, stomatal behavior in all treatments and conditions was similar to that observed at 3 DAD (Figure 5A), excepting control plants exposed to drought, in which it was not possible to take leaf samples due to the wilt phenotype of the plants.

To correlate the HB-mediated stomatal closure upon drought conditions with the water content of tomato plants, we also measured the fresh weight at 3 and 6 DAD. At 6 DAD, control-treated plants under drought conditions showed an approximately 50% reduction in the fresh weight. Nevertheless, in the case of HB-treated plants, no statistically significant differences were observed between well-watered plants and those that were under water deficit conditions (Figure 5B).

Finally, plasma membrane damage was also evaluated by measuring electrolyte leakage. In severe drought conditions (6 DAD), no significant differences were observed between HB-treated plants. However, control-treated plants subjected to drought displayed a higher percentage of ion leakage than the rest of treatments, suggesting the role of HB in cell membrane protection and stabilization (Figure 5C). Nonetheless, no differences were found between treatments and conditions related to chlorophyll content, indicating that water-stressed plants had a withered appearance, but they were not completely collapsed (Supplemental Figure 3).

To further analyze the mode of action of HB in an ABA-independent manner, water deprivation experiments were carried out in *flc* mutant plants (Supplemental Figure 4). Due to ABA-deficient plants wilt phenotype, samples were only taken at 3 DAD since they were collapsed at 6 DAD. As we previously observed (Figure 5A), stomatal closure in HB-treated WT plants was similar to non-treated WT plants subjected to drought. Besides, HB treatments in *flacca* plants slightly triggered stomatal closure (Supplemental Figure 4A), confirming the previous results observed in disc treatments (Figure 2). Regarding weight loss, no significant differences were found (Supplemental Figure 4B). Our results suggest that HB treatments conferred drought tolerance in tomato plants in an ABA-independent manner.

Tomato plants treated with HB show lower proline content under drought conditions

To better understand the role of HB in drought tolerance, proline biosynthesis and accumulation were analyzed, since proline is a well-known osmoprotectant (Ozturk et al., 2021). As expected, tomato non-treated plants that were subjected to water deprivation accumulated higher proline levels than well-watered plants. However, when

HB-treated plants were analyzed, no statistical differences were found between non-stressed and water-stressed plants (Figure 6A).

Remarkably, a similar trend was observed regarding proline biosynthesis, in which Δ^1-Pyrroline-5-Carboxylate Synthetase 1 (P5CS1) is the rate-limiting enzyme (Gonzalez-Guzman et al., 2014; Kaur & Asthir 2015). We observed that tomato *P5CS1* gene (*Solyc06g01970*) expression was significantly induced under drought conditions in both HB and non-treated plants. Nevertheless, *P5CS1* expression was lower in the case of HB-treated plants and the expression level was statistically similar to watered, non-treated plants (Figure 6B). Therefore, HB effect appears to alleviate the drought stress, since mechanisms counteracting against the water deprivation are less activated in HB-treated plants.

Transcriptomic changes in HB treatments under water stress revealed a repression of ABA biosynthesis

To provide insight into the molecular responses of the plants exposed to HB subjected or not to water deprivation, a further RNA-seq analysis was performed. A gene clustering analysis with DEGS from both RNA-seq (DEG threshold= 2), was performed for discovering groups of correlated genes between different treatments (non-treated and HB-treated) and conditions (well-watered and non-watered plants). Following this approach, 16 clusters were generated (Supplemental Figure 5). According to cluster trends we grouped them in 3 groups of interest: first DEGS that share the same response to HB in well-watered and non-watered conditions (clusters 7, 10, 12 and 16), second DEGS that only respond to HB in non-abiotic stress conditions (clusters 5 and 6) and third DEGS that only respond to HB in water deficit conditions (clusters 2 and 3). To elucidate the function of these three groups of genes, a GO enrichment analysis for biological processes was executed. Interestingly, no GO term was enriched in the first group that share the same response in both watering conditions. Regarding DEGs that only respond after HB treatments in well-watered conditions (clusters 5 and 6), we found GO terms related to apocarotenoid and abscisic acid metabolism, which correlated well with the previously observed results indicating that the HB mode of action was independent of ABA (Figure 7A).

To further study the relationship between HB and ABA, DEGS that only respond to HB in well-watered conditions from the enriched category related to abscisic acid metabolic processes (GO:0009687), previously cited were identified. This set has 3 genes that were involved in different critical steps of ABA biosynthesis, like 9-cis-epoxycarotenoid

dioxygenase (NCED; Solyc07g056570), zeaxanthin epoxidase (Solyc02g090890), and ABA 8'-hydroxylase (Solyc04g078900). The pattern of expression of these genes was analyzed by RT-qPCR, observing a tendency of down-regulation upon HB treatments in watered plants, that confirms their behavior in the RNA-seq (Figures 7B, 7C and 7D). Since our results revealed a down-regulation of genes involved in ABA biosynthesis, we explored the levels of ABA accumulation in HB-treated or non-treated, and well-watered or non-watered plants. In our experiments, we did not observe significant differences in ABA content between non- and HB-treated plants under well-watered conditions. Surprisingly, we observed that water-stressed plants treated with HB significatively accumulated less ABA than the stressed untreated plants, being levels similar to those observed in non-stressed plants (Figure 7E). Also, we analyzed the expression of marker genes of ABA signaling (Gonzalez-Guzman et al., 2014), such as Responsive to ABA 18 (*RAB18*), the transcription factor *MYB44,* and a *late embryogenesis abundant* (*LEA*) protein in tomato plants at 6 DAD. Drought treatment induced the expression levels of *RAB18* and *LEA* in non- and HB-treated plants. Interestingly, *LEA* gene induction in HB-treated plants was higher than in non-treated plants for both watered and drought stress conditions (Supplemental Figure 6). The higher induction of *LEA* in water-stressed plants treated with HB (Supplemental Figure 6) which accumulate lower levels of ABA (Figure 7E) appears to reinforce that HB induces the abiotic response in an ABA-independent manner.

HB application improves productivity under water-limiting conditions

A high yield is a crucial factor for profitable crop production. For this reason, we considered whether drought tolerance conferred by HB treatments in tomato plants could contribute to improve productivity. To this end, we carried out treatments in an experimental field located in Pincanya (Spain) under limited water availability (50 %).

On one hand, we examined tomato fruits setting along the experimental trial. As Figure 8A shows, water stressed HB-treated plants developed significantly more flowers than non-treated plants almost during all the experimental trial. Related to this, we detected a set of genes involved in flower development that were altered by HB treatments under drought conditions in the RNA-seq analysis (Supplemental Figure 7). Besides, the observed higher amount in flowers turned into higher fruit yield set at 12 DA-F (Days After treatment F, See Materials and Methods) (Figure 8B). On the other hand, we assessed the number of fruits and total productivity at different time points. At the beginning of the harvesting period, the number of fruits in HB-treated plants was lower

than non-treated plants. However, from the fifth harvest (14 DA-H), the number of fruits in HB-treated plants became similar to the untreated tomato plants. At the end of the harvesting period, HB treatments produced higher yield (23%) than non-treated plants (Figure 8C). Furthermore, the same trend was observed regarding fruit weight (Figure 8D), thus indicating that periodic HB treatments can improve tomato fruit size and productivity under drought conditions. The harvested fruits were also classified depending on their size into extra, class I, class II or class III. Both fruit weight and fruit number were higher in the extra and class I groups, in tomato plants treated with HB subjected to drought conditions (Supplemental Figure 8). Our results indicate that HB treatments increase productivity and quality of the fruits in water-stressed tomato plants.

HB treatments lead to pathogen resistance

Since HB application activates defense-related genes and confers resistance to the bacteria *Pst* DC3000 under greenhouse conditions with controlled inoculations (López-Gresa et al., 2018), experimental trials were carried out to assess whether HB defensive effects have potential uses in agriculture. The first trial was performed to confirm the agricultural applications of HB in tomato plants against *Pst* DC3000. For this purpose, tomato plants were treated periodically with different HB concentrations (0.05, 5,10 and 50 mM), using the commercial pesticide OXICOOP 50 as positive control. The applications started as preventive and were performed as a broadcast foliar application on the tomato plants before appearance of bacterial disease symptoms (see Materials and Methods). On each assessment date, the percentage of leaves presenting symptoms per plot (incidence) and the leaf area infected (severity) were evaluated on 10 plants per plot. At the beginning of the experiment, HB-treated plants did not show differences with respect to untreated plants in the percentage of severity or incidence of the bacterial infection. Nonetheless, at 0 DA-C and 8 DA-C intermediate and high concentrations of HB acted in a similar way to the commercial pesticide OXICOOP 50, being the efficacy of incidence between 68 and 78% for high dose of HB treatments and between 77-81% at last assessment considering percentage of infected leaf (Figure 9).

Furthermore, we tested the efficacy of HB in a different plant-pathogen interaction in which stomatal immunity is crucial, that is potato defense against *Phytophthora infestans*. For this end, the same approach as tomato against *Pst* field trial was followed but employing OROCOBRE as a commercial positive control treatment.

Regarding the percentage of damaged leaf area, all plots showed statistical differences compared to the untreated control check since 6 DA-D. The best results were obtained with the 500 mM HB treatment, reaching efficacies near to 70% at the end of trial, surpassing the performance of the reference OROCOBRE which efficacy was around 52% at the end of trial (Figures 10A and 10B). Regarding symptomatology in potato plants, HB treatments showed statistical significances since the beginning of the trial, obtaining similar efficacy on downy mildew incidence than treatments with the commercial fungicide (Figures 10C and 10D).

Therefore, our results indicated that HB can be efficiently used to prevent diseases in agriculture caused by pathogens whose entrance is through stomata.

Discussion

Climate change is one on the greatest challenges of our time. The impacts of climate change are affecting crop production and increasing pressure on natural ecosystems and resources (FAO, 2022). Abiotic stresses, including drought, heat, or salinity, together with biotic stresses, represent the major threats for crop yield so new different strategies are emerging to increase crop adaptation for future climatic conditions. One of the most powerful and promising alternatives for crop protection is related with the exploitation of plant defense responses (Alagna *et al.*, 2020). Plants have developed a two-tier accurate and sophisticated innate immune system, consisting of PTI mediated by PRRs, and NLRs-mediated ETI for detecting pathogenic effectors (Jones and Dangl, 2006). Although the two defensive barriers involve different activation mechanisms, PTI and ETI converge into many similar downstream responses although the kinetics and amplitude of the responses are different (Tsuda & Katagiri 2010; Yuan et al., 2021). The shared defense signaling network is mainly composed by the activation of MAPKs, ROS production, Ca^{2+} influx, activation/inhibition of ion channels and transcriptomic reprogramming which causes the accumulation of secondary metabolites to manage stress. Plant innate immune machinery also involves the rapid closure of stomata, a response known as stomatal immunity, in order to restrict pathogen invasion (Melotto et al., 2006).

In previous studies, we identified different GLVs that were emitted when tomato plants efficiently resisted bacterial infection with *Pst*. Particularly, the volatile HB stood out due to its properties as a stomatal closure compound and defense-related gene inducer, but the detailed mechanisms of HB in plant immunity still remain undeciphered

(López-Gresa et al., 2018). In this work, a transcriptomic analysis revealed that HB treatments triggered the activation of different processes that were related to plant defense mechanisms such as chitin catabolism, glucosamine and aminoglycan metabolism or endopeptidase activity, re-confirming the HB-mediated defensive genes induction (Figure 1A, and Supplemental Figure 1).

The role of stomata as active defensive barriers in plant immunity has been extensively studied. Specifically, in the infections caused by *Pst* DC3000*,* bacterial flagellin epitope flg22 triggers stomata closure through the recognition by the receptor complex FLS2-BAK1, the subsequent NADPH oxidase-dependent ROS production and the activation of MAPK signaling cascades, mainly via MPK3 and MPK6 (Chinchilla et al., 2007; Beckers et al., 2009; Li et al., 2014). Furthermore, ABA biosynthesis and signaling are essential to stomatal immunity (Melotto et al., 2006; Du et al., 2014; Su et al., 2017). However, it has been demonstrated that PAMPs- and ABA-mediated stomatal immunity pathways are independent. Contrary to PAMP-mediated stomatal closure, ABA signaling pathway leads to ROS production via the Open Stomata 1 (OST1) kinase, that leads to MPK9 and MPK12 activation, triggering ABA-mediated stomata closure (Jammes et al., 2009, 2011; Montillet et al., 2013; Su et al., 2017). Besides, both phytohormones ABA and jasmonate, the signaling pathways of which are often exploited by pathogens, transcriptionally activate a common family of protein phosphatases that suppress immune-associated MPK3 and MPK6 kinases (Mine *et al.*, 2017). Our results showed that HB treatments induce stomatal closure as effectively as ABA and flg22, although higher concentrations of HB were applied to obtain similar aperture sizes as ABA treatment (Supplemental Figure 2). Nonetheless, HB treatments in ABA-deficient mutants triggered stomatal closure (Figure 2A), demonstrating that HB-mediated stomatal closure is ABA-independent. Moreover, chemical approaches also indicated that, similarly to flg22, HB treatments induced stomatal closure and plant defense signaling trough NADPH-oxidase ROS production and Ca^{2+} ion permeable channels (Figures 2, B, C and D). Furthermore, we have also observed that MPK3 and MPK6 activation is essential for HB-triggered stomatal immunity (Figure 3). Our results correlate with other studies that have shown that GLV exposure induced the activation of these downstream responses. For instance, exposure of Arabidopsis plants to (*E*)-2-hexenal and (*E*)-2-hexenol involved membrane potential depolarization through an increase in cytosolic Ca^{2+} via ROS-activated calcium channels (Asai *et al.*, 2009). Besides, maize and Arabidopsis plants exposed to (*Z*)-3-hexenol and (*E*)-2-hexenal, respectively, increased the transcript abundance of different genes involved in defense signaling (Engelberth, Contreras, Dalvi, Li & Engelberth 2013; Mirabella et al., 2015).

The facts that GLVs are formed from plant endogenous components, they are emitted upon pathogen infection, and exogenous application activate defense signaling mechanisms suggest that GLVs, and particularly HB, can act as DAMPs (Duran-Flores and Heil, 2016). DAMPs are danger signals released by plants upon pathogen attack that have a relevant role amplifying the immune responses.

Drought is considered as one of the most significant factors limiting crop productivity, and new strategies are needed to cope with this global threat (Konapala *et al.*, 2020). In response to drought stress conditions, the first option for plants is to partially close stomata to prevent water loss via transpiration (Torres-Ruiz et al., 2013; Clauw et al., 2015; Pirasteh-Anosheh, Saed-Moucheshi, Pakniyat & Pessarakli 2016). In this study, we have shown that stomatal aperture ratio of HB-treated tomato plants was similar to the stomatal aperture ratio of plants that were subjected to water stress (Figure 5A), a phenomenon that led to minimize weight loss and ion leakage after 6 days of water deprivation (Figures 5 B and C), indicating that HB-mediated stomatal closure was also effective in drought. Besides, the HB-treatments under both irrigation and drought conditions did not penalize the plant in terms of chlorophyll content (Supplemental Figure 3). It was also noteworthy that HB application under drought conditions highly induced the expression of a *LEA* family genes (Supplemental Figure 6C), which are thought to participate in membrane protein stability, osmotic adjustment and macromolecular stabilization (Jiang & Huang 2002; Ling, Zeng & Guo 2016; Ozturk et al., 2021) denoting that HB-mediated drought tolerance in tomato plants could be not only due to stomatal closure, but also due to the role of HB as an osmoprotectant compound. In fact, some mechanisms that balance out the water deprivation, such as proline biosynthesis and accumulation, are less activated in HB-treated plants (Figure 6).

ABA is a pivotal hormone governing plant response to drought. Under limited water availability conditions, plants show the induction of ABA biosynthetic enzymes, such as 9-cis-epoxycarotenoid dioxygenase (NCED1*),* that result in high levels of ABA accumulation (Dar et al., 2017). In the same manner than in biotic stress experiments, interconnection between HB and ABA was studied in *flc* mutants, thus exogenous HB application in *flc* mutants subjected to water deficit confirmed that HB-meditated stomatal closure under drought conditions was independent of ABA biosynthesis (Supplemental Figure 4). Moreover, the transcriptomic analysis of non- and HB-treated tomato plants under normal or water stress conditions revealed that HB application down-regulated the expression of different ABA *de novo* biosynthetic genes, as zeaxanthin epoxidase (Solyc02g090890) and 9-cis-epoxycarotenoid dioxygenase

(Solyc07g056570) and catabolism genes like ABA 8'-hydroxylase (Solyc04g078900) (Figure 7) that are dominant contributors to ABA homeostasis in Arabidopsis and tomato plants (Burbidge *et al.*, 1999; Iuchi *et al.*, 2001; Saito *et al.*, 2004; Kushiro *et al.*, 2004). This gene repression correlated with the low accumulation of ABA in HB-treated plants compared to non-treated under drought conditions (Figure 7E). These results, together with the high induction of *LEA* family genes, lower levels of proline accumulation and *P5C1* gene expression in water stressed HB-treated plants (Figure 6), appear to indicate that drought stress mechanisms were not activated in HB-treated plants, suggesting that HB signaling is interfering in ABA homeostasis. All these data suggests that HB alleviates drought stress in tomato plants mainly due to HB-induced stomatal closure.

The application of osmoprotectans and biostimulants as elicitors to confer plant tolerance to different biotic and abiotic stresses through priming is a promising alternative to conventional techniques. The priming mechanism enables plants to respond more robustly and rapidly, which results in an enhanced resistance or tolerance to a stress condition (Beckers & Conrath, 2007; Conrath et al., 2006; Alagna et al., 2020). Most-know priming compounds are synthetic SA analogs, such as (1,2,3) thiadiazole-7-carbothioic acid S-methyl ester (BTH) or 2,6-dichloroisonicotinic acid and its methyl ester (both referred to as INA) which trigger the activation of systemic acquired resistance (SAR), and the non-protein amino acid β-aminobutyric acid (BABA) that protects plants against various biotic and abiotic stresses in a plethora of plant species (Kohler et al., 2002; Bektas & Eulgem, 2015; Jisha & Puthur, 2016; Martínez-Aguilar et al., 2016; Thevenet et al., 2017). Many VOCs have also been described as elicitors and priming compounds. Hexanoic acid can activate broad-spectrum defenses by inducing callose deposition and activating SA and JA signaling pathways. Besides, its efficiency has been demonstrated in a wide range of host plants and pathogens (Aranega-Bou et al., 2014; Llorens et al., 2016). Another example of VOCs as priming agents against abiotic factors is the GLV (Z)-3-hexenyl acetate, since maize seeds primed with this volatile exhibited cold tolerance (Cofer et al., 2018). In greenhouse conditions, our laboratory demonstrated the induction of resistance against bacterial infection of a similar compound, (Z)-3-hexenyl butyrate (HB), through stomata closure (López-Gresa et al., 2018). In this study, the enhanced resistance to pathogens and tolerance to drought conditions caused by the HB has also been demonstrated in field conditions. Regular exogenous HB treatments in tomato plants under limited water availability conditions resulted in greater number and size of tomato fruits compared to non-treated plants (Figures 8 B, C and D; Supplemental Figure 6). HB efficacy in field

was also demonstrated in the previously analyzed tomato-bacteria interaction and also against potato late blight caused by Phytophthora infestans, obtaining in both cases highest efficacies than commercial agrochemicals (Figures 9 and 10) with the added advantage of being non-toxic unlike most conventional pesticides. According to these results, HB is proposed as a promising natural elicitor compound against biotic and abiotic stress.

In summary, the results obtained in this work provide evidence for the role of HB in stomatal immunity in tomato and Arabidopsis plants, being ROS generation by NADPH oxidases, Ca2+ fluxes, MPK3/6 activation, but not ABA, essential for HB-mediated stomatal immunity. Moreover, HB-induced stomatal closure resulted in enhanced resistance and tolerance to pathogen infection and drought in field conditions, proposing HB as a novel natural elicitor candidate and a promising strategy for sustainable agriculture.

Supplementary data

Supplemental Figure 1. Validation of RNA-seq data by RT-qPCR.

Supplemental Figure 2. Dose-response (A) and time course (B) analysis of HB, flg22 and ABA in tomato leaves stomatal aperture.

Supplemental Figure 3. Effect of HB treatments on chlorophyll content in tomato leaves

Supplemental Figure 4. Effect of HB treatments in ABA-deficient mutants.

Supplemental Figure 5. Cluster analysis of RNAseq data of tomato plants under different treatments (+/-HB) and conditions (+/-$H_2$0).

Supplemental Figure 6. ABA-related gene expression profiles in tomato plants treated with HB.

Supplemental Figure 7. Heat map of flowering related genes from the RNA-seq from non-watered plants experiment.

Supplemental Figure 8. Total yield per categories in tomato plants upon HB treatments under open field conditions.

Supplemental Table 1. Primer sequences used for quantitative RT-PCR analysis of the selected tomato genes.

Acknowledgements

We would like to thank Químicas Meristem (Valencia, Spain), especially to Dr. Giovanni Pensabene for her excellent technical support in the open field assays.

Author contributions

MPL-G and PL designed the research; CP, BB-P, FV and JPP performed research; LJ, FV and JPP contributed RNA-Seq analytic tools; CP, BB-P, FV JPP, LJ, IR, JMB, MPL-G and PL analyzed and discussed data; CP, MPL-G and PL wrote the paper and incorporated the input of the rest of the authors.

Conflict of interest

No conflict of interest is declared.

Funding

This work was supported by Grant PID2020-116765RB-I00 funded by MCIN/ AEI/10.13039/501100011033/ and Grant CDTI/IDI-20200721 funded by MCIN/ Químicas Meristem S.L. Work in the lab is also supported by grant PROMETEU/2021/056 by Generalitat Valenciana. C.P. was a recipient of a predoctoral contract of the Generalitat Valenciana (ACIF/2019/187), J.P-P is a recipient of a predoctoral contract of the Ministerio de Universidades e Investigacion (FPU21/00259), and B.B-P was a recipient of a postdoctoral contract of the Ministerio de Universidades (Ayuda María Zambrano para la Atracción de Talento Internacional).

References

Abbott WS. 1925. A Method of Computing the Effectiveness of an Insecticide. Journal of Economic Entomology **18**, 265–267.

Alagna F, Balestrini R, Chitarra W, Marsico AD, Nerva L. 2020. *Getting ready with the priming: Innovative weapons against biotic and abiotic crop enemies in a global changing scenario*. Elsevier Inc.

Ameye M, Audenaert K, De Zutter N, Steppe K, Van Meulebroek L, Vanhaecke L, De Vleesschauwer D, Haesaert G, Smagghe G. 2015. Priming of wheat with the

green leaf volatile Z-3-hexenyl acetate enhances defense against Fusarium Graminearum but boosts deoxynivalenol production. Plant Physiology **167**, 1671–1684.

Aranega-Bou P, de la O Leyva M, Finiti I, Garcfa-Agustfn P, Gonzalez-Bosch C. 2014. Priming of plant resistance by natural compounds. Hexanoic acid as a model. Frontiers in Plant Science **5**.

Arnaud D, Hwang I. 2015. A sophisticated network of signaling pathways regulates stomatal defenses to bacterial pathogens. Molecular Plant **8**, 566–581.

Asai N, Nishioka T, Takabayashi J, Furuichi T. 2009. Plant volatiles regulate the activities of Ca2+ -permeable channels and promote cytoplasmic calcium transients in Arabidopsis leaf cells. Plant signaling & behavior **4**, 294–300.

Baldwin IT, Halitschke R, Paschold A, Von Dahl CC, Preston CA. 2006. Volatile signaling in plant-plant interactions: 'Talking trees' in the genomics era. Science **311**, 812–815.

Beckers GJM, Conrath U. 2007. Priming for stress resistance: from the lab to the field. Current Opinion in Plant Biology **10**, 425–431.

Beckers GJM, Jaskiewicz M, Liu Y, Underwood WR, He SY, Zhang S, Conrath U. 2009. Mitogen-Activated protein kinases 3 and 6 are required for full priming of stress responses in Arabidopsis thaliana. Plant Cell **21**, 944–953.

Bektas Y, Eulgem T. 2015. Synthetic plant defense elicitors. Frontiers in Plant Science **5**, 1–9.

Bharath P, Gahir S, Raghavendra AS. 2021. Abscisic Acid-Induced Stomatal Closure: An Important Component of Plant Defense Against Abiotic and Biotic Stress. Frontiers in Plant Science **12**, 1–18.

Bjornson M, Pimprikar P, Nürnberger T, Zipfel C. 2021. The transcriptional landscape of Arabidopsis thaliana pattern-triggered immunity. Nature plants **7**, 579–586.

Boutrot F, Zipfel C. 2017. Function, Discovery, and Exploitation of Plant Pattern Recognition Receptors for Broad-Spectrum Disease Resistance. Annual Review of Phytopathology **55**, 257–286.

Brilli F, Loreto F, Baccelli I. 2019. Exploiting plant volatile organic compounds (VOCS) in agriculture to improve sustainable defense strategies and productivity of crops. Frontiers in Plant Science **10**, 1–8.

Burbidge A, Grieve TM, Jackson A, Thompson A, McCarty DR, Taylor IB. 1999.

Characterization of the ABA-deficient tomato mutant notabilis and its relationship with maize Vp14. The Plant Journal **17**, 427–431.

Campos L, Lisón P, López-Gresa MP, Rodrigo I, Zacarés L, Conejero V, Bellés JM. 2014. Transgenic tomato plants overexpressing tyramine N-hydroxycinnamoyltransferase exhibit elevated hydroxycinnamic acid amide levels and enhanced resistance to Pseudomonas syringae. Molecular plant-microbe interactions□: MPMI **27**, 1159–1169.

Chinchilla D, Bauer Z, Regenass M, Boller T, Felix G. 2006. The Arabidopsis receptor kinase FLS2 binds flg22 and determines the specificity of flagellin perception. Plant Cell **18**, 465–476.

Chinchilla D, Zipfel C, Robatzek S, Kemmerling B, Nürnberger T, Jones JDG, Felix G, Boller T. 2007. A flagellin-induced complex of the receptor FLS2 and BAK1 initiates plant defence. Nature **448**, 497–500.

Chong L, Xu R, Ku L, Zhu Y. 2022. Beyond stress response: OST1 opening doors for plants to grow. Stress Biology **2**, 44.

Clauw P, Coppens F, De Beuf K, Dhondt S, Van Daele T, Maleux K, Storme V, Clement L, Gonzalez N, Inzé D. 2015. Leaf Responses to Mild Drought Stress in Natural Variants of Arabidopsis . Plant Physiology **167**, 800–816.

Cofer TM, Engelberth M, Engelberth J. 2018. Green leaf volatiles protect maize (Zea mays) seedlings against damage from cold stress. Plant Cell and Environment **41**, 1673–1682.

Conrath U, Beckers GJM, Flors V, *et al.* 2006. Priming: Getting ready for battle. Molecular Plant-Microbe Interactions **19**, 1062–1071.

Cui H, Tsuda K, Parker JE. 2015. Effector-triggered immunity: From pathogen perception to robust defense. Annual Review of Plant Biology **66**, 487–511.

Dar NA, Amin I, Wani W, Wani SA, Shikari AB, Wani SH, Masoodi KZ. 2017. Abscisic acid: A key regulator of abiotic stress tolerance in plants. Plant Gene **11**, 106–111.

Du M, Zhai Q, Deng L, *et al.* 2014. Closely related NAC transcription factors of tomato differentially regulate stomatal closure and reopening during pathogen attack. Plant Cell **26**, 3167–3184.

Dudareva N, Klempien A, Muhlemann JK, Kaplan I. 2013. Biosynthesis, function and metabolic engineering of plant volatile organic compounds. New Phytologist **198**,

16–32.

Duran-Flores D, Heil M. 2016. Sources of specificity in plant damaged-self recognition. Current Opinion in Plant Biology **32**, 77–87.

Engelberth J, Contreras CF, Dalvi C, Li T, Engelberth M. 2013. Early Transcriptome Analyses of Z-3-Hexenol-Treated Zea mays Revealed Distinct Transcriptional Networks and Anti-Herbivore Defense Potential of Green Leaf Volatiles. PLOS ONE **8**, e77465.

FAO. 2022. *Crops and climate change impact briefs*.

Gómez-Gómez L, Boller T. 2000. FLS2: An LRR receptor-like kinase involved in the perception of the bacterial elicitor flagellin in Arabidopsis. Molecular Cell **5**, 1003–1011.

Gonzalez-Guzman M, Rodriguez L, Lorenzo-Orts L, *et al.* 2014. Tomato PYR/PYL/RCAR abscisic acid receptors show high expression in root, differential sensitivity to the abscisic acid agonist quinabactin, and the capability to enhance plant drought resistance. Journal of Experimental Botany **65**, 4451–4464.

Hahn A, Harter K. 2009. Mitogen-activated protein kinase cascades and ethylene: Signaling, biosynthesis, or both? Plant Physiology **149**, 1207–1210.

Heil M, Bueno JCS. 2007. Within-plant signaling by volatiles leads to induction and priming of an indirect plant defense in nature. Proceedings of the National Academy of Sciences of the United States of America **104**, 5467–5472.

Iuchi S, Kobayashi M, Taji T, Naramoto M, Seki M, Kato T, Tabata S, Kakubari Y, Yamaguchi-Shinozaki K, Shinozaki K. 2001. Regulation of drought tolerance by gene manipulation of 9-cis-epoxycarotenoid dioxygenase, a key enzyme in abscisic acid biosynthesis in Arabidopsis. The Plant Journal **27**, 325–333.

Jammes F, Song C, Shin D, *et al.* 2009. MAP kinases MPK9 and MPK12 are preferentially expressed in guard cells and positively regulate ROS-mediated ABA signaling. Proceedings of the National Academy of Sciences of the United States of America **106**, 20520–20525.

Jammes F, Yang X, Xiao S, Kwak JM. 2011. Two arabidopsis guard cell-preferential MAPK genes, MPK9 and MPK12, function in biotic stress response. Plant Signaling and Behavior **6**, 1875–1877.

Jiang Y, Huang B. 2002. Protein Alterations in Tall Fescue in Response to Drought Stress and Abscisic Acid. Crop Science **42**, 202–207.

Jisha KC, Puthur JT. 2016. Seed Priming with Beta-Amino Butyric Acid Improves

Abiotic Stress Tolerance in Rice Seedlings. Rice Science **23**, 242–254.

Jones JDG, Dangl JL. 2006. The plant immune system. Nature **444**, 323–329.

Kadota Y, Sklenar J, Derbyshire P, *et al.* 2014. Direct Regulation of the NADPH Oxidase RBOHD by the PRR-Associated Kinase BIK1 during Plant Immunity. Molecular Cell **54**, 43–55.

Kaur G, Asthir B. 2015. Proline: a key player in plant abiotic stress tolerance. Biologia Plantarum **59**, 609–619.

Kim D, Langmead B, Salzberg SL. 2015. HISAT: a fast spliced aligner with low memory requirements. Nature methods **12**, 357–360.

Kohler A, Schwindling S, Conrath U. 2002. Benzothiadiazole-induced priming for potentiated responses to pathogen infection, wounding, and infiltration of water into leaves requires the NPR1/NIM1 gene in Arabidopsis. Plant Physiology **128**, 1046–1056.

Konapala G, Mishra AK, Wada Y, Mann ME. 2020. Climate change will affect global water availability through compounding changes in seasonal precipitation and evaporation. Nature Communications **11**, 3044.

Kovaka S, Zimin A V., Pertea GM, Razaghi R, Salzberg SL, Pertea M. 2019. Transcriptome assembly from long-read RNA-seq alignments with StringTie2. Genome Biology **20**, 1–13.

Kushiro T, Okamoto M, Nakabayashi K, Yamagishi K, Kitamura S, Asami T, Hirai N, Koshiba T, Kamiya Y, Nambara E. 2004. The Arabidopsis cytochrome P450 CYP707A encodes ABA 8'-hydroxylases: key enzymes in ABA catabolism. The EMBO journal **23**, 1647–1656.

Li L, Li M, Yu L, *et al.* 2014. The FLS2-associated kinase BIK1 directly phosphorylates the NADPH oxidase RbohD to control plant immunity. Cell Host and Microbe **15**, 329–338.

Ling H, Zeng X, Guo S. 2016. Functional insights into the late embryogenesis abundant (LEA) protein family from Dendrobium officinale (Orchidaceae) using an Escherichia coli system. Scientific Reports **6**, 39693.

Llorens E, Camañes G, Lapeña L, García-Agustín P. 2016. Priming by hexanoic acid induce activation of mevalonic and linolenic pathways and promotes the emission of plant volatiles. Frontiers in Plant Science **7**, 1–12.

López-Gresa MP, Lisón P, Campos L, Rodrigo I, Rambla JL, Granell A, Conejero

V, Bellés JM. 2017. A non-targeted metabolomics approach unravels the VOCs associated with the tomato immune response against Pseudomonas syringae. Frontiers in Plant Science **8**, 1–15.

López-Gresa MP, Payá C, Ozáez M, Rodrigo I, Conejero V, Klee H, Bellés JM, Lisón P. 2018. A new role for green leaf volatile esters in tomato stomatal defense against pseudomonas syringe pv. Tomato. Frontiers in Plant Science **871**, 1–12.

Luna E. 2016. Using green vaccination to brighten the agronomic future. Outlooks on Pest Management **27**, 136–140.

Mao G, Meng X, Liu Y, Zheng Z, Chen Z, Zhang S. 2011. Phosphorylation of a WRKY transcription factor by two pathogen-responsive MAPKs drives phytoalexin biosynthesis in Arabidopsis. Plant Cell **23**, 1639–1653.

Martínez-Aguilar K, Ramírez-Carrasco G, Hernández-Chávez JL, Barraza A, Alvarez-Venegas R. 2016. Use of BABA and INA As activators of a primed state in the common bean (Phaseolus vulgaris L.). Frontiers in Plant Science **7**, 1–17.

Melotto M, Underwood W, Koczan J, Nomura K, He SY. 2006. Plant Stomata Function in Innate Immunity against Bacterial Invasion. Cell **126**, 969–980.

Mi H, Muruganujan A, Huang X, Ebert D, Mills C, Guo X, Thomas PD. 2019. Protocol Update for large-scale genome and gene function analysis with the PANTHER classification system (v.14.0). Nature protocols **14**, 703–721.

Mine A, Berens ML, Nobori T, Anver S, Fukumoto K, Winkelmüller TM, Takeda A, Becker D, Tsuda K. 2017. Pathogen exploitation of an abscisic acid- and jasmonate-inducible MAPK phosphatase and its interception by Arabidopsis immunity. Proceedings of the National Academy of Sciences of the United States of America **114**, 7456–7461.

Mirabella R, Rauwerda H, Allmann S, Scala A, Spyropoulou EA, de Vries M, Boersma MR, Breit TM, Haring MA, Schuurink RC. 2015. WRKY40 and WRKY6 act downstream of the green leaf volatile E-2-hexenal in Arabidopsis. The Plant Journal **83**, 1082–1096.

Montillet JL, Leonhardt N, Mondy S, *et al.* 2013. An Abscisic Acid-Independent Oxylipin Pathway Controls Stomatal Closure and Immune Defense in Arabidopsis. PLoS Biology **11**, 13–15.

Mustilli AC, Merlot S, Vavasseur A, Fenzi F, Giraudat J. 2002. Arabidopsis OST1 protein kinase mediates the regulation of stomatal aperture by abscisic acid and acts upstream of reactive oxygen species production. Plant Cell **14**, 3089–3099.

Ozturk M, Turkyilmaz Unal B, García-Caparrós P, Khursheed A, Gul A, Hasanuzzaman M. 2021. Osmoregulation and its actions during the drought stress in plants. Physiologia Plantarum **172**, 1321–1335.

Payá C, Pilar López-Gresa M, Intrigliolo DS, Rodrigo I, Bellés JM, Lisón P. 2020. (Z)-3-hexenyl butyrate induces stomata closure and ripening in vitis vinifera. Agronomy **10**.

Pertea M, Kim D, Pertea GM, Leek JT, Salzberg SL. 2016. Transcript-level expression analysis of RNA-seq experiments with HISAT, StringTie and Ballgown. Nature Protocols **11**, 1650–1667.

Pertea M, Pertea GM, Antonescu CM, Chang TC, Mendell JT, Salzberg SL. 2015. StringTie enables improved reconstruction of a transcriptome from RNA-seq reads. Nature Biotechnology **33**, 290–295.

Pirasteh-Anosheh H, Saed-Moucheshi A, Pakniyat H, Pessarakli M. 2016. Stomatal responses to drought stress. Water Stress and Crop Plants, 24–40.

Raudvere U, Kolberg L, Kuzmin I, Arak T, Adler P, Peterson H, Vilo J. 2019. G:Profiler: A web server for functional enrichment analysis and conversions of gene lists (2019 update). Nucleic Acids Research **47**, W191–W198.

Saito S, Hirai N, Matsumoto C, Ohigashi H, Ohta D, Sakata K, Mizutani M. 2004. Arabidopsis CYP707As encode (+)-abscisic acid 8'-hydroxylase, a key enzyme in the oxidative catabolism of abscisic acid. Plant physiology **134**, 1439–1449.

Su J, Zhang M, Zhang L, Sun T, Liu Y, Lukowitz W, Xu J, Zhang S. 2017. Regulation of stomatal immunity by interdependent functions of a pathogen-responsive MPK3/MPK6 cascade and abscisic acid. Plant Cell **29**, 526–542.

Tal M. 1966. Abnormal Stomatal Behavior in Wilty Mutants of Tomato. Plant Physiology **41**, 1387–1391.

Taylor IB, Linforth RST, Al-Naieb RJ, BowmanWR, Marples BA. 1988. The wilty tomato mutants flacca and sitiens are impaired in the oxidation of ABA-aldehyde to ABA. Plant, Cell & Environment **11**, 739–745.

Thevenet D, Pastor V, Baccelli I, Balmer A, Vallat A, Neier R, Glauser G, Mauch-Mani B. 2017. The priming molecule β-aminobutyric acid is naturally present in plants and is induced by stress. New Phytologist **213**, 552–559.

Torres-Ruiz JM, Diaz-Espejo A, Morales-Sillero A, Martín-Palomo MJ, Mayr S, Beikircher B, Fernández JE. 2013. Shoot hydraulic characteristics, plant water status

and stomatal response in olive trees under different soil water conditions. Plant and Soil **373**, 77–87.

Tsuda K, Katagiri F. 2010. Comparing signaling mechanisms engaged in pattern-triggered and effector-triggered immunity. Current Opinion in Plant Biology **13**, 459–465.

Vahisalu T, Kollist H, Wang Y-F, *et al.* 2008. SLAC1 is required for plant guard cell S-type anion channel. Nature **452**, 487–491.

Wang W, Feng B, Zhou JM, Tang D. 2020. Plant immune signaling: Advancing on two frontiers. Journal of Integrative Plant Biology **62**, 2–24.

Wang Y, Schuck S, Wu J, Yang P, Döring AC, Zeier J, Tsuda K. 2018. A mpk3/6-wrky33-ald1-pipecolic acid regulatory loop contributes to systemic acquired resistance[open]. Plant Cell **30**, 2480–2494.

Yuan M, Ngou BPM, Ding P, Xin XF. 2021. PTI-ETI crosstalk: an integrative view of plant immunity. Current Opinion in Plant Biology **62**, 102030.

Zhang J, Zhou JM. 2010. Plant immunity triggered by microbial molecular signatures. Molecular Plant **3**, 783–793.

Zhou J, Wang J, Zheng Z, Fan B, Yu JQ, Chen Z. 2015. Characterization of the promoter and extended C-terminal domain of Arabidopsis WRKY33 and functional analysis of tomato WRKY33 homologues in plant stress responses. Journal of Experimental Botany **66**, 4567–4583.

Figure Legends

Figure 1. Transcriptomic analysis confirms the role of HB in plant immunity. Functional profiling analysis of upregulated (A) and downregulated (B) DEGs between HB- and control-treated plants.

Figure 2. HB-mediated stomatal closure requires Ca^{2+} signaling and ROS production by NADPH oxidases, but not ABA biosynthesis. (A) Lukullus (WT) and *flacca* tomato leaf discs were floated on liquid MS for 3 h under light. Then, 1 μM flg22, 10 μM ABA and 50 μM HB were applied and stomatal aperture ratio was determined 2 h after treatments. In the case of chemical inhibitors experiments, 2 mM EGTA **(B),** 20 μM DPI **(C)** and 2 mM SHAM **(D)** were added in MoneyMaker tomato leaf discs before elicitors treatments. Violin plots represent the stomatal aperture ratio of 50 stomata for each treatment. Different letters

indicate statistically significant differences for each genotype and treatment ($P < 0.05$, two-way ANOVA with Tukey HSDTest)

Figure 3. Activation of MPK3 and MPK6 is involved in HB-mediated stomatal immunity. MPK activation assay in tomato **(A)** and *Arabidopsis thaliana* **(B)** leaf discs 15, 30 and 60 minutes after treatments with 1 μM flg22, 10 μM ABA and 50 μM HB. MPK activation was detected by immunoblot analysis using the Phospho-p44/42 MAPK (Erk1/2; Thr-202/Tyr204) rabbit monoclonal antibody. Western blot experiments were performed three times and yielded similar results. **(C)** Stomatal aperture ratio was measured in tomato leaf discs floated on MS liquid for 3 h under light, pre- treated with the MPKs inhibitor PD98059 20 μM and followed by treatments with 1 μM flg22, 10 μM ABA and 50 μM HB for 2 h. **(D)** Growth of *Pst* on tomato leaves of control (-HB) and HB-treated (+HB) after treatments with the MPKs inhibitor PD98059. Plants were sprayed with with PD98059 100 μM for 3 hours, subsequently treated with HB 5 μM or water for 24 h into methacrylate chambers, and then dip inoculated with *Pst*. Bacterial growth measurements were done 24 h after inoculation. **(E)** Stomatal aperture ratio of Arabidopsis Col-0, *mpk3* and *mpk6* mutants leaf discs 2 h after treatments with flg22, ABA and HB. **(F)** Growth of *Pst* on *Arabidopsis thaliana* leaves of control (-HB) and HB-treated (+HB) 3 days after inoculation. Plants were treated with HB 5 μM or water for 24 h into methacrylate chambers, and then infected by spray with *Pst*. In stomatal aperture experiments, 50 stomata were measured per each treatment and condition (violin plots). Data correspond to at least four independent plants ±□SEM of a representative experiment. Statistically significant differences are represented by different letters ($P < 0.05$, two-way ANOVA with Tukey HSD).

Figure 4. HB treatments induce MPK3/6-mediated downstream signaling. Real-time qPCR analysis of *WRKY33A* **(A),** *WRKY33B* **(B),** *ETR4* **(C)** and an ethylene responsive factor (*ERF)* **(D)** gene expression in HB-treated plants. Expression levels are relative to tomato mock plants and normalized to the tomato actin gene. Data represent the mean of three independent plants ± SEM. Asterisk (*) and double asterisks (**) indicate statistically significant differences with $P \leq 0.05$ and $P \leq 0.01$, respectively (Student's *t*-test).

Figure 5. HB treatments induce tolerance to drought in tomato plants. Differences related to stomatal aperture ratio **(A)**, weight **(B)** and ion leakage **(C)** in tomato plants treated (+HB) or not (-HB) with HB, in normal (+$H_2$0) or water stressed conditions (-$H_2$0). Samples were taken after 3 or 6 days after exposure (DAD) to

drought conditions. Data in (B) and (C) correspond to six independent plants ±□SEM of a representative experiment. 50 stomata were measured per each treatment and condition (violin plots). Different letters indicate statistically significant differences for each genotype and treatment ($P < 0.05$, two-way ANOVA with Tukey HSD).

Figure 6. Tomato plants treated with HB have lower proline content under drought conditions. Tomato plants were periodically sprayed (+HB) or not (-HB) with 2 mM HB, and plants were subjected (-$H_2$0) or not (+$H_2$0) to 6 days of water deprivation. **(A)** Tomato leaves proline content. Data correspond to averages of six independent plants ±□SEM of a representative experiment. **(B)** *P5CS1* gene relative expression. RT-qPCR values were normalized with the level of expression of the actin gene. Bars represent the mean ± SEM of a representative experiment. Different letters indicate statistically significant differences for each genotype and treatment ($P < 0.05$, two-way ANOVA with Tukey HSD).

Figure 7. ABA biosynthetic pathway is repressed by HB treatments. Plants were treated (+HB) or not (-HB) with HB 2 mM and were subjected to water deprivation (-$H_2$0) for 6 days or normally watered (+$H_2$0). **(A)** Functional analysis profiling of RNA-Seq data comparing different treatments (+/-HB) and conditions (+/-$H_2$0). Real-time qPCR analysis of *Solyc02g056570* **(B),** *Solyc02g09890* **(C)** and *Solyc04g078900* **(D)** genes. Expression levels are relative to tomato non-treated and watered plants and normalized to the tomato actin gene. **(D)** ABA accumulation in tomato leaves upon different treatments and conditions. Data correspond to the averages of three independent plants ± SEM of a representative experiment. Different letters indicate statistically significant differences for each genotype and treatment ($P < 0.05$, two-way ANOVA with Tukey HSD).

Figure 8. HB treatments in tomato plants improve productivity under drought conditions in open field experiments. Number of flowers **(A),** number of set fruits **(B),** total harvested fruits **(C)** and mean fruit weight **(D)** of tomato plants under limited water availability conditions (50%) and treated (+HB) or not (-HB) with 5mM HB. Time units are referred as follows: X DA Z, being X day (0-18); DA Days After; Z day of treatment (A-H). Points represent mean values. Different letters indicate significant differences at each time point ($P < 0.05$, two-way ANOVA with Tukey HSD).

Figure 9. HB application enhances resistance to *Pseudomonas syringae* in tomato plants. Percentage of **(A)** severity, **(B)** efficacy on severity, **(C)** incidence

and **(D)** efficacy on incidence of untreated plants, HB weekly-treated plants at different concentrations (0.05, 5, 10 ,50 mM) and plants treated with OXICOOP 50. Time units are referred as follows: X DA Z, being X day (0-8); DA Days After; Z day of treatment (A-C). An ANOVA test was performed, and different letters indicate statistical significances with a *P*-value < 0.05.

Figure 10. HB treatments confer resistance to the oomycete *Phytophthora infestans* in potato plants under open field conditions. Percentage of **(A)** severity, **(B)** efficacy on severity, **(C)** incidence and **(D)** efficacy on incidence of untreated plants, HB weekly-treated plants at different concentrations (0.05, 5, 50, 500 mM) and plants treated with OXICOOP 50. Time units are referred as follows: X DA Z, being X day (0-27); DA Days After; Z day of treatment (A-D). An ANOVA test was performed, and different letters indicate statistical significances with a *P*-value < 0.05.

Supplemental Figure 1. Validation of RNA-seq data by RT-qPCR. 4 weeks-old tomato plants were treated (+HB) or not (-HB) with 5 μM HB into methacrylate chambers. Gene expression analysis of the *PR1* (X68738), *PR5* (X70787), a pathogen recognition receptor (Solyc12g036793), plant cadmium resistance 2 (Solyc06g066590) and chlorophyll binding genes (Solyc06g069730; Solyc06g069000; Solyc12g011280) was examined by RT-qPCRs using total RNA from leaves. The RT-qPCR values were normalized with the level of expression of the actin gene. Data represent the mean ± SEM of a representative experiment (n=4). Double (**) and triple (***) asterisks indicate significant differences between treatments with *P*-value < 0.01 and *P*-value < 0.001, respectively (Student's *t*-test).

Supplemental Figure 2. Dose-response (A) and time course (B) analysis of HB, flg22 and ABA in tomato leaves stomatal aperture. Data represent the mean ±□SEM of a representative experiment (n=50). Different letters indicate statistically significant differences for each treatment at each time point (*P* < 0.05, one-way ANOVA with Tukey HSD Test).

Supplemental Figure 3. Effect of HB treatments in tomato leaves chlorophyll content. Chlorophyll a, chlorophyll b and total chlorophyll content in tomato plants treated (+HB) or not (-HB) with HB, in normal (+H2O) or water stressed conditions (-H2O). Data correspond to six independent plants ±□SEM of a representative experiment. No statistically significant differences were found.

Supplemental Figure 4. Effect of HB treatments in ABA-deficient mutants. Differences related to stomatal aperture ratio **(A)** and weight **(B)** in Lukullus (WT) and *flaca (flc)* tomato plants treated (+HB) or not (-HB) with HB, in normal (+H_20) or water stressed conditions (-H_20). Samples were taken after 3 days after exposure to drought conditions. Bars represent the mean ±□SEM of a representative experiment (n=6). In stomatal aperture assays, 50 stomata were measured in each treatment and conditions (violin plots). Statistically significant differences are represented by different letters with *P*-value < 0.05.

Supplemental Figure 5. Cluster analysis of RNAseq data of tomato plants under different treatments (+/-HB) and conditions (+/-H_20). Plants were treated (+HB) or not (-HB) with HB 2 mM and were subjected to water deprivation (-H_20) for 6 days or normally watered (+H_20). Blue lines correspond to HB treatments relative expression in water conditions, and black lines represent expression data from plants subjected to drought.

Supplemental Figure 6. ABA-related genes expression profiles in tomato plants treated with HB. Plants were treated with HB (+HB) or water (-HB) periodically. Water-stressed plants were subjected to water deficit for 6 days. *RAB18* **(A),** *MYB44* **(B)** and *LEA* family **(C)** gene relative expression in plants under normal (+H_20) or water deficit conditions (-H_20). Gene expression analysis were examined by RT-qPCRs using total RNA from leaves. The RT-qPCR values were normalized with the level of expression of the actin gene. Bars represent the mean ± the standard deviation of a representative experiment (n=3). Different letters indicate statistically significant differences for each treatment and condition (*P* < 0.05, one-way ANOVA with Tukey HSD Test).

Supplemental Figure 7. Heat map of flowering related genes from the RNA-seq from non-watered plants experiment. The numbers in each box represent the ratio between the fragments per kilobase of exon per million mapped fragments (FPKM) of each replicated divided the average of the FPKM from the six individual samples.

Supplemental Figure 8. Total yield per categories in tomato plants upon HB treatments under open field conditions. Tomato plants were subjected to water limitation (50%) and treated (+HB) or not (-HB) with HB. Number of harvested fruits **(A)** and total weight of harvested fruits **(B)** per categories were analyzed as follows: small size (25-50 mm diameter, 25-100 g weight); medium size (50-75 mm diameter,100-200 g weight); big size (75-100 mm diameter, 200-300 g

weight); and extra size (>100 mm diameter, >300 g weight).

Supplemental Table 1. Primer sequences used for quantitative RT-PCR analysis of the selected tomato genes.

Supplemental Table 2. List of genes after cluster analysis with DEGS from RNA-seq analysis.

Figure 1

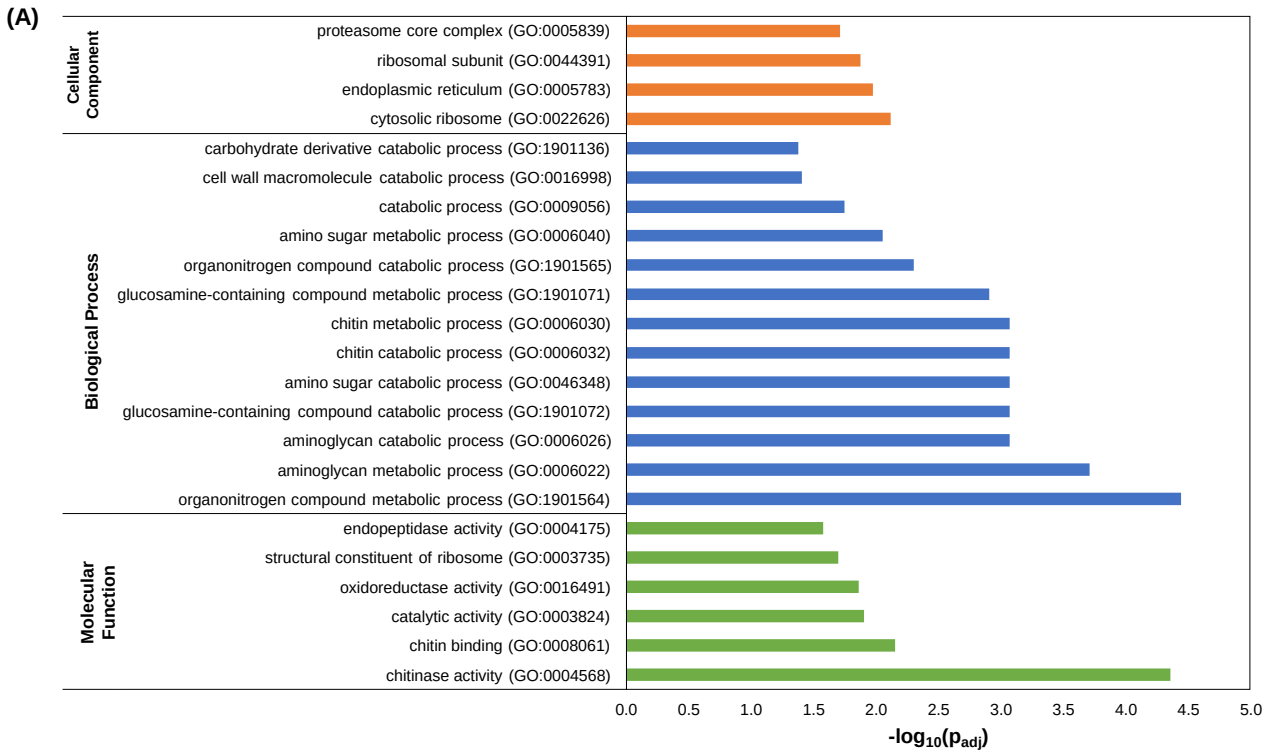

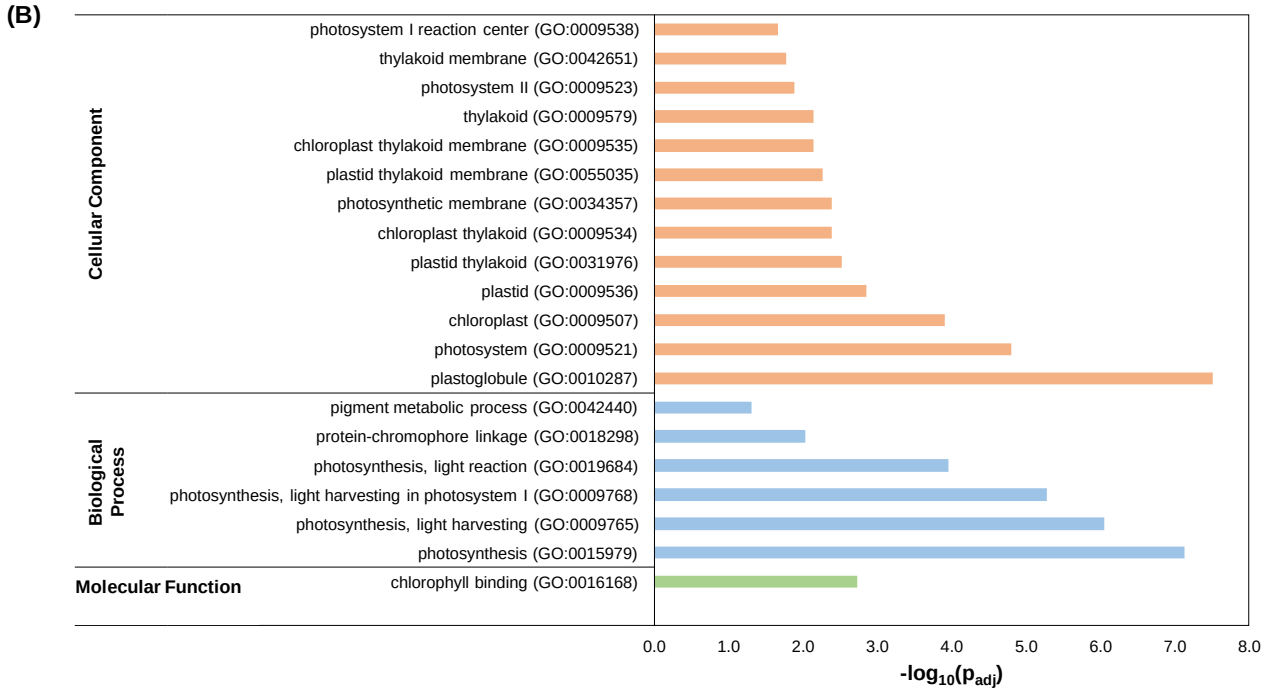

Figure 1. Transcriptomic analysis confirms the role of HB in plant immunity. Functional profiling analysis of upregulated (A) and downregulated (B) DEGs between HB- and control-treated plants.

Figure 2

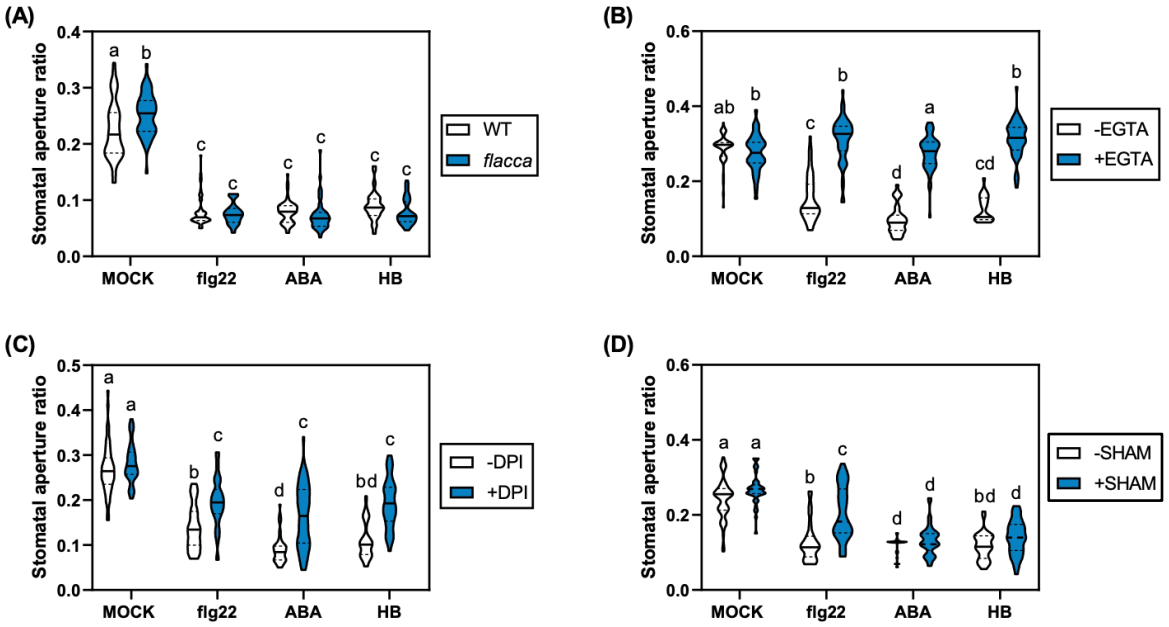

Figure 2. HB-mediated stomatal closure requires Ca^{2+} signaling and ROS production by NADPH oxidases, but not ABA biosynthesis. (A) Lukullus (WT) and *flacca* tomato leaf discs were floated on liquid MS for 3 h under light. Then, 1 µM flg22, 10 µM ABA and 50 µM HB were applied and stomatal aperture ratio was determined 2 h after treatments. In the case of chemical inhibitors experiments, 2 mM EGTA **(B),** 20 µM DPI **(C)** and 2 mM SHAM **(D)** were added in MoneyMaker tomato leaf discs before elicitors treatments. Violin plots represents the stomatal aperture ratio of 50 stomata for each treatment. Different letters indicate statistically significant differences for each genotype and treatment ($P < 0.05$, two-way ANOVA with Tukey HSDTest).

Figure 3

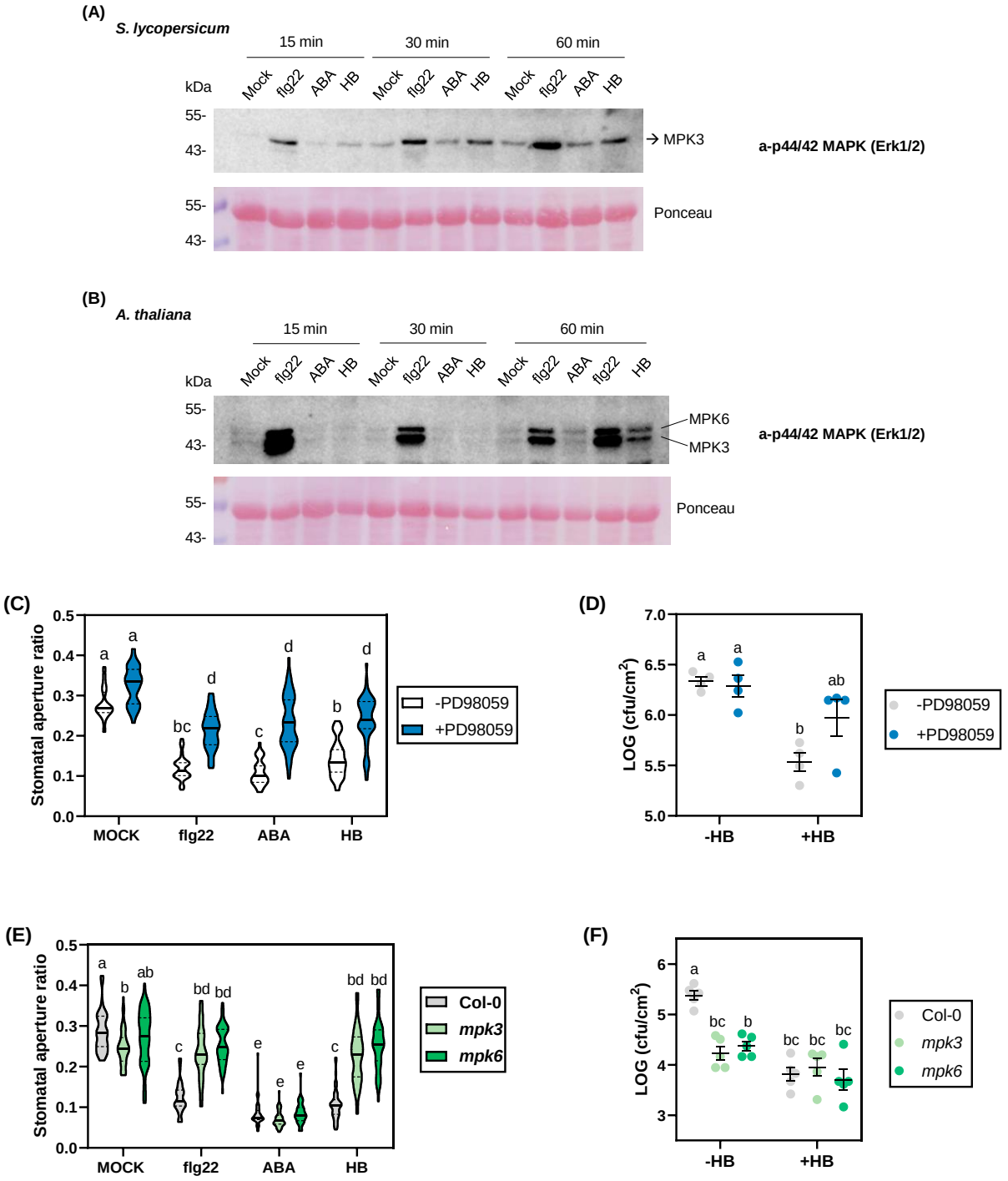

Figure 3. Activation of MPK3 and MPK6 is involved in HB-mediated stomatal immunity. MPK activation assay in tomato **(A)** and Arabidopsis thaliana **(B)** leaf discs 15, 30 and 60 minutes after treatments with 1 µM flg22, 10 µM ABA and 50 µM HB. MPK activation was detected by immunoblot analysis using the Phospho-p44/42 MAPK (Erk1/2; Thr-202/Tyr204) rabbit monoclonal antibody. Western blot experiments were performed three times and yielded similar results. **(C)** Stomatal aperture ratio was measured in tomato leaf discs floated on MS liquid for 3 h under light, pre-treated with the MPKs inhibitor PD98059 20 µM and followed by treatments with 1 µM flg22, 10 µM ABA and 50 µM HB for 2 h. **(D)** Growth of *Pst* on tomato leaves of control (-HB) and HB-treated (+HB) after treatments with the MPKs inhibitor PD98059. Plants were sprayed with with PD98059 100 µM for 3 hours, subsequently treated with HB 5 µM or water for 24 h into methacrylate chambers, and then dip inoculated with *Pst*. Bacterial growth measurements were done 24 h after inoculation. **(E)** Stomatal aperture ratio of Arabidopsis Col-0, *mpk3* and *mpk6* mutants leaf discs 2 h after treatments with flg22, ABA and HB. **(F)** Growth of *Pst* on *Arabidopsis thaliana* leaves of control (-HB) and HB-treated (+HB) 3 days after inoculation. Plants were treated with HB 5 µM or water for 24 h into methacrylate chambers, and then infected by spray with *Pst* . In stomatal aperture experiments, 50 stomata were measured per each treatment and condition (violin plots). Data correspond to at least four independent plants ± SEM of a representative experiment. Statistically significant differences are represented by different letters ($P < 0.05$, two-way ANOVA with Tukey HSD).

Figure 4

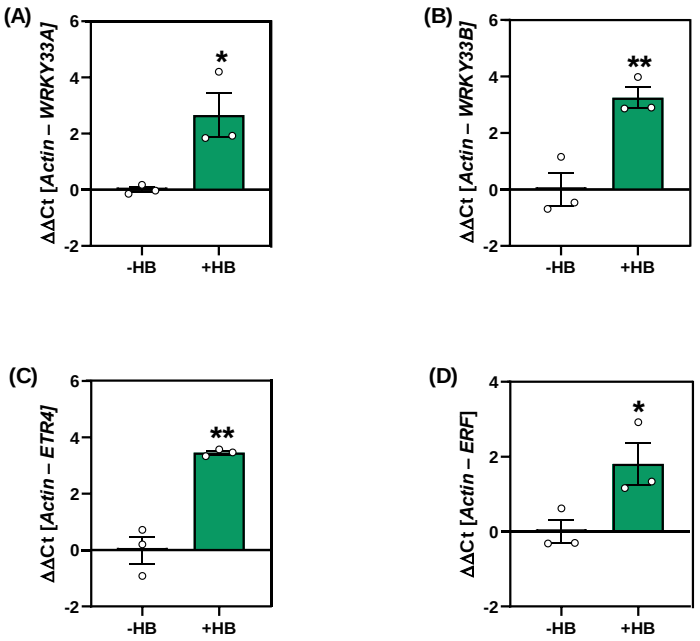

Figure 4. HB treatments induce MPK3/6-mediated downstream signaling. Real-time qPCR analysis of *WRKY33A* **(A),** *WRKY33B* **(B),** *ETR4* **(C)** and an ethylene responsive factor (*ERF)* **(D)** gene expression in HB-treated plants. Expression levels are relative to tomato mock plants and normalized to the tomato actin gene. Data represent the mean of three independent plants ± SEM. Asterisk (*) and double asterisks (**) indicate statistically significant differences with $P \leq 0.05$ and $P \leq 0.01$, respectively (Student's *t*-test).

Figure 5

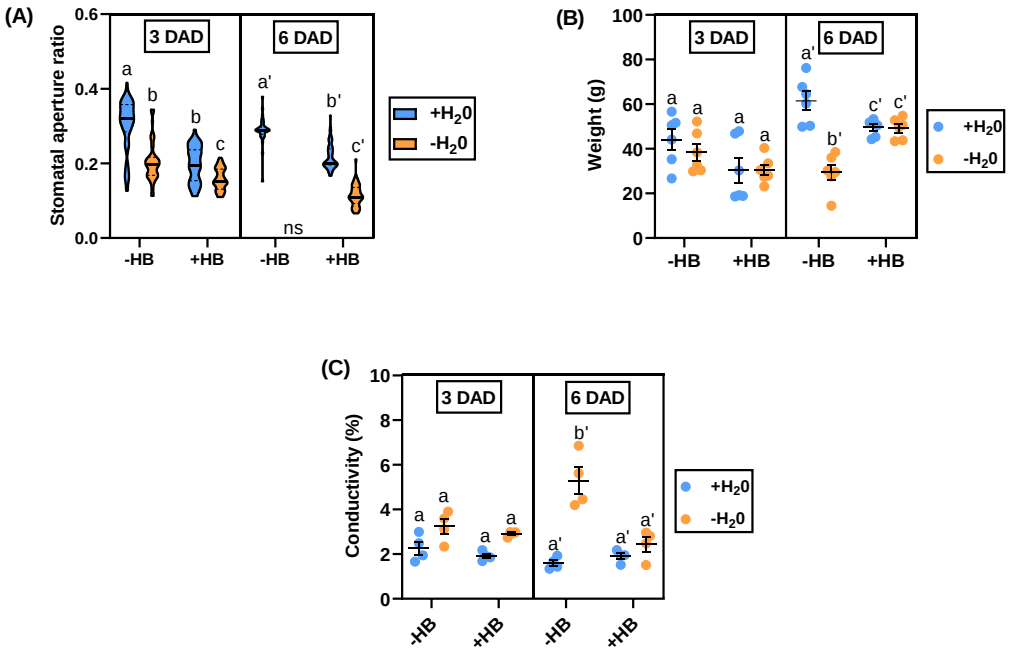

Figure 5. HB treatments induce tolerance to drought in tomato plants. Differences related to stomatal aperture ratio **(A)**, weight **(B)** and ion leakage **(C)** in tomato plants treated (+HB) or not (-HB) with HB, in normal (+H_20) or water stressed conditions (-H_20). Samples were taken 3 or 6 days after exposure (DAD) to drought conditions. Data in (B) and (C) correspond to six independent plants ± SEM of a representative experiment. 50 stomata were measured per each treatment and condition (violin plots). Different letters indicate statistically significant differences for each genotype and treatment ($P < 0.05$, two-way ANOVA with Tukey HSD).

Figure 6

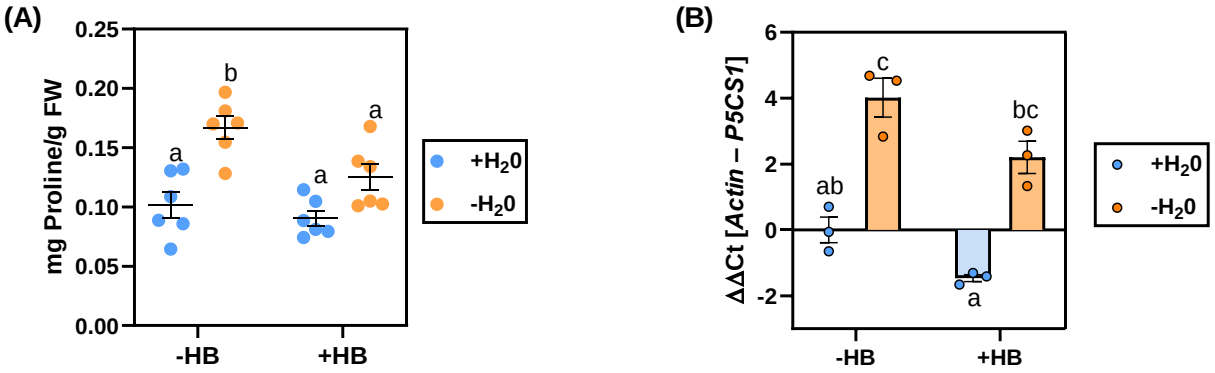

Figure 6. Tomato plants treated with HB have lower proline content under drought conditions. Tomato plants were periodically sprayed (+HB) or not (-HB) with 2 mM HB, and plants were subjected (-H_20) or not (+H_20) to 6 days of water deprivation. **(A)** Tomato leaves proline content. Data correspond to averages of six independent plants ± SEM of a representative experiment. **(B)** *P5CS1* gene relative expression. RT-qPCR values were normalized with the level of expression of the actin gene. Bars represent the mean ± SEM of a representative experiment. Different letters indicate statistically significant differences for each genotype and treatment ($P < 0.05$, two-way ANOVA with Tukey HSD).

Figure 7

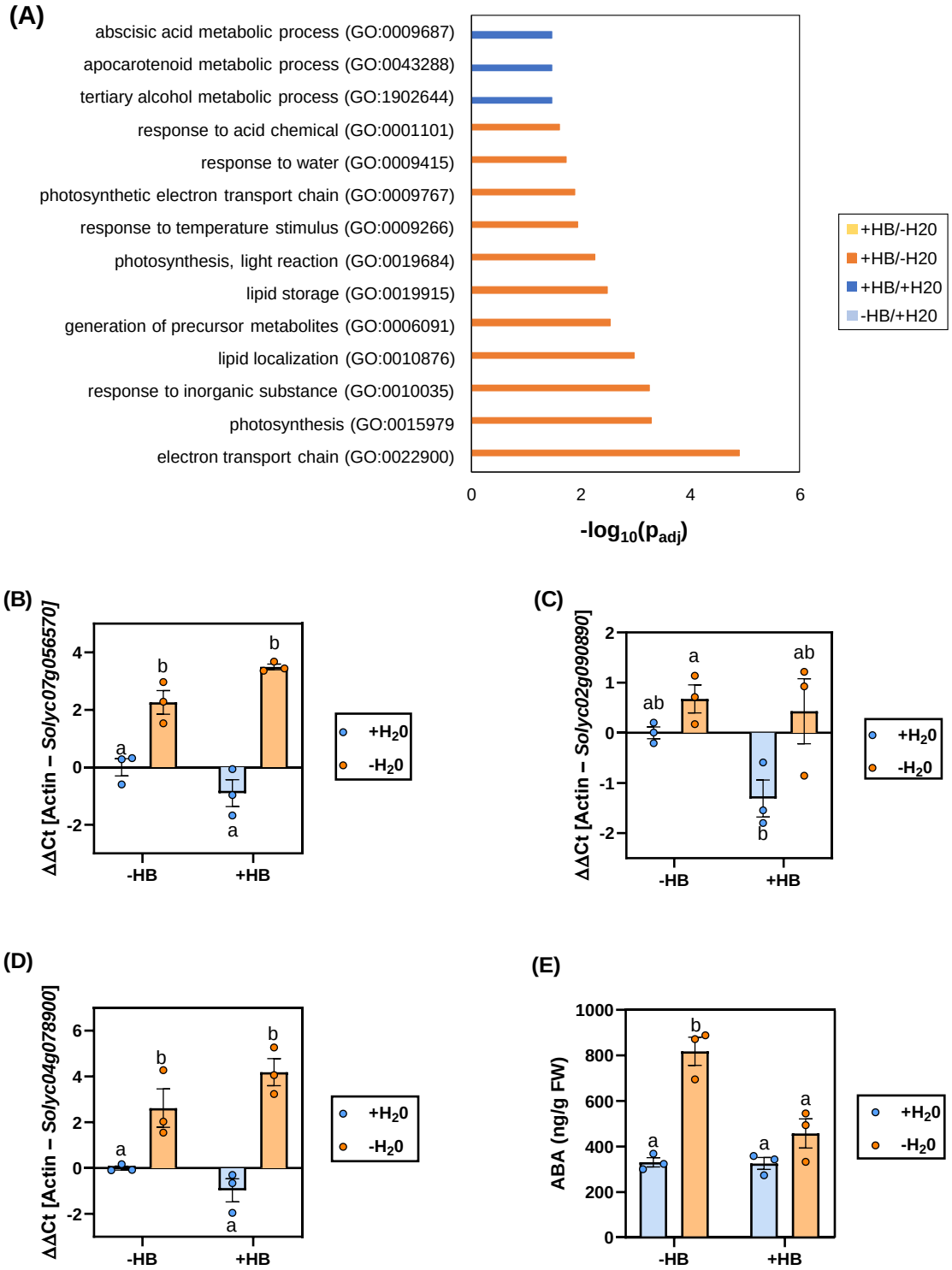

Figure 7. ABA biosynthetic pathway is repressed by HB treatments. Plants were treated (+HB) or not (-HB) with 2 mM HB and were subjected to water deprivation (-$H_2$0) for 6 days or normally watered (+$H_2$0). **(A)** Functional analysis profiling of RNA-Seq data comparing different treatments (+/-HB) and conditions (+/-$H_2$0). Real-time qPCR analysis of *Solyc07g056570* **(B),** *Solyc02g09890* **(C)** and *Solyc04g078900* **(D)** genes. Expression levels are relative to tomato non-treated and watered plants and normalized to the tomato actin gene. **(D)** ABA accumulation in tomato leaves upon different treatments and conditions. Data correspond to the averages of three independent plants ± SEM of a representative experiment. Different letters indicate statistically significant differences for each genotype and treatment ($P < 0.05$, two-way ANOVA with Tukey HSD).

Figure 8

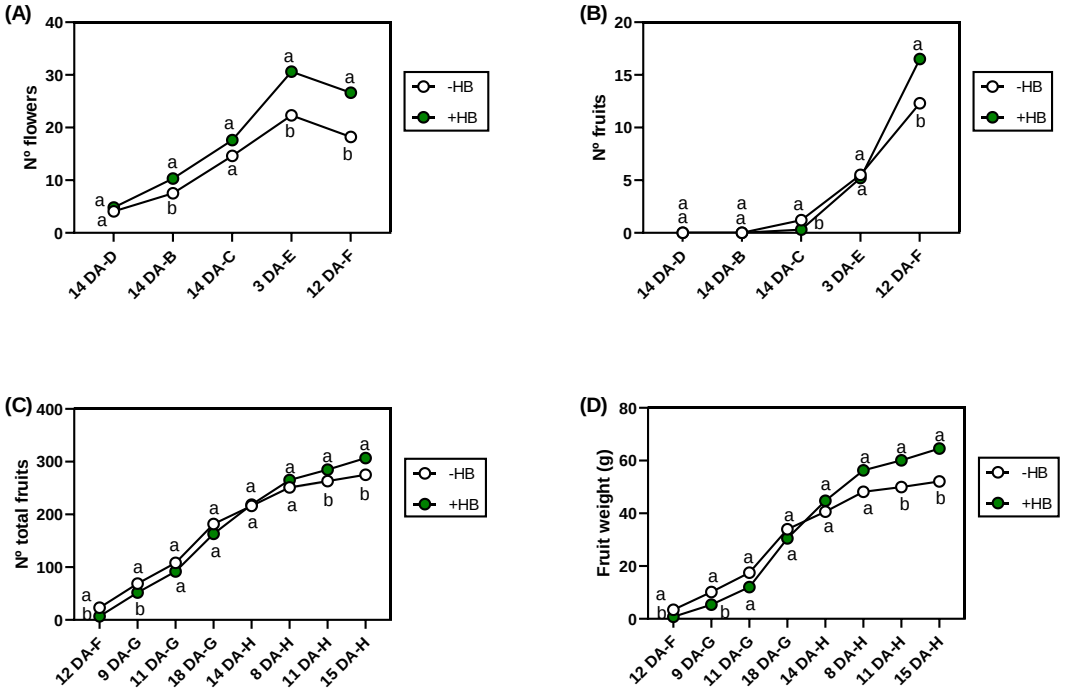

Figure 8. HB treatments in tomato plants improve productivity under drought conditions in open field experiments. Number of flowers **(A),** number of set fruits **(B),** total harvested fruits **(C)** and mean fruit weight **(D)** of tomato plants under limited water availability conditions (50%) and treated (+HB) or not (-HB) with 5mM HB. Time units are referred as follows: X DA Z, being X day (0-18); DA Days After; Z day of treatment (A-H). Points represent mean values. Different letters indicate significant differences at each time point ($P < 0.05$, two-way ANOVA with Tukey HSD).

Figure 9

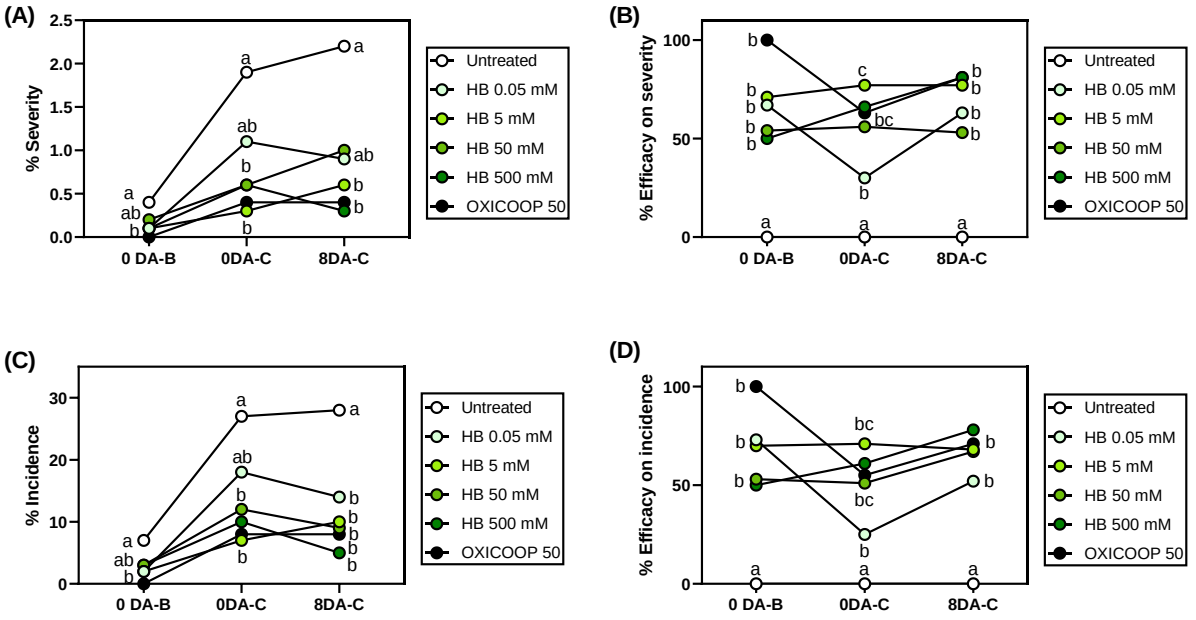

Figure 9. HB application enhances resistance to *Pseudomonas syringae* in tomato plants. Percentage of severity **(A)**, efficacy on severity **(B)**, incidence **(C)** and efficacy on incidence **(D)** of untreated plants, HB weekly-treated plants at different concentrations (0.05, 5, 10, 50 mM) and plants treated with OXICOOP 50. Time units are referred as follows: X DA Z, being X day (0-8); DA Days After; Z day of treatment (A-C). An ANOVA test was performed, and different letters indicate statistical significances with a *P*-value < 0.05.

Figure 10

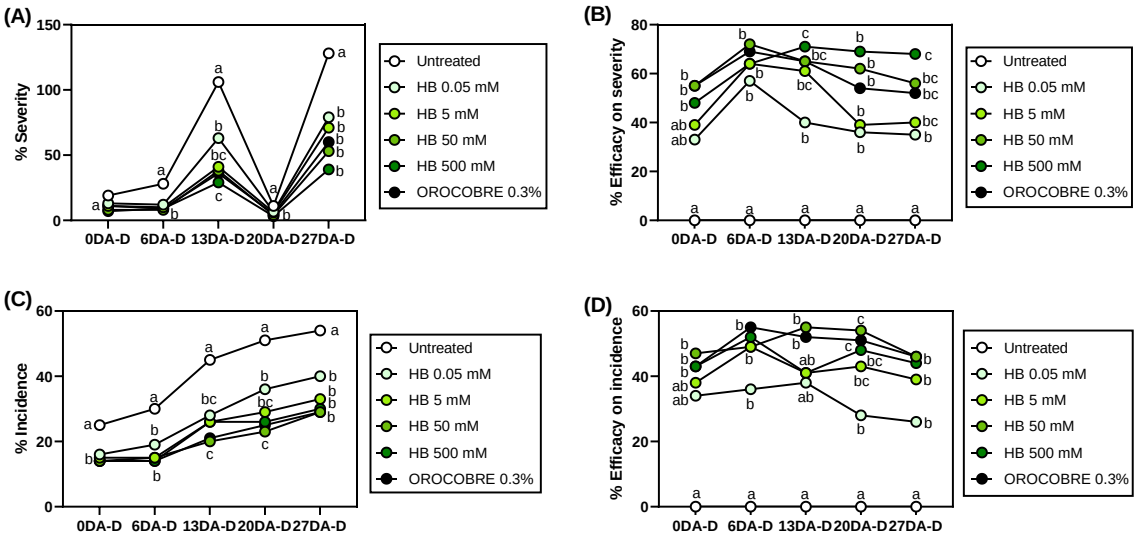

Figure 10. HB treatments confer resistance to the oomycete *Phytophthora infestans* in potato plants under open field conditions. Percentage of **(A)** severity, **(B)** efficacy on severity, **(C)** incidence and **(D)** efficacy on incidence of untreated plants, HB weekly-treated plants at different concentrations (0.05, 5, 50, 500 mM) and plants treated with OXICOOP 50**.** Time units are referred as follows: X DA Z, being X day (0-27); DA Days After; Z day of treatment (A-D). An ANOVA test was performed, and different letters indicate statistical significances with a $P < 0.05$.